

Delay Alignment Modulation with Hybrid Analog/Digital Beamforming for Millimeter Wave and Terahertz Communications

Jieni Zhang, Yong Zeng, *Senior Member, IEEE*, Xiangbin Yu, *Senior Member, IEEE*, Shi Jin, *Fellow, IEEE*, Jinhong Yuan, *Fellow, IEEE*, Ying-Chang Liang, *Fellow, IEEE*, and Rui Zhang, *Fellow, IEEE*

Abstract—For millimeter wave (mmWave) or Terahertz (THz) communications, by leveraging the high spatial resolution offered by large antenna arrays and the multi-path sparsity of mmWave/THz channels, a novel inter-symbol interference (ISI) mitigation technique called delay alignment modulation (DAM) has been recently proposed. The key ideas of DAM are *delay pre-compensation* and *path-based beamforming*. However, existing research on DAM is mainly based on fully digital beamforming, which requires the number of radio frequency (RF) chains to be equal to the number of antennas. This paper proposes the hybrid analog/digital beamforming based DAM, including both fully and partially connected structures. The analog and digital beamforming matrices are designed to achieve performance close to DAM based on fully digital beamforming. While DAM was considered for the path-based channel model with integer delays in the previous work, this paper extends DAM to a more general tap-based model that accounts for fractional path delays. To further reduce the cost of channel estimation and improve the performance for wireless channels with fractional delays, DAM with codebook-based beam alignment and DAM-orthogonal frequency division multiplexing (DAM-OFDM) with hybrid beamforming are proposed. The effectiveness of the proposed techniques is verified by extensive simulation results.

Index Terms—delay alignment modulation (DAM), hybrid beamforming, codebook-based beam alignment, DAM-OFDM.

I. INTRODUCTION

Over the years, there has been an increasing demand for high-capacity data transmission, catalyzing extensive research into massive multiple-input multiple-output (MIMO) or even extremely large-scale MIMO (XL-MIMO) systems [1], especially when integrated with millimeter-wave (mmWave) and Terahertz (THz) communication technologies [2], [3].

Part of this work has been presented at the IEEE WCNC 2023 [54].

Jieni Zhang, Yong Zeng, and Shi Jin are with the National Mobile Communication Research Laboratory, Southeast University, Nanjing 210096, China; Yong Zeng is also with the Purple Mountain Laboratories, Nanjing 211111, China (e-mail: {220230984, yong_zeng, jinshi}@seu.edu.cn). (*Corresponding author: Yong Zeng.*)

Xiangbin Yu is with the College of Electronic and Information Engineering, Nanjing University of Aeronautics and Astronautics, Nanjing 210016, China (e-mail: yxbxwy@gmail.com).

Jinhong Yuan is with the School of Electrical Engineering and Telecommunications, The University of New South Wales, Sydney, NSW 2052, Australia (e-mail: j.yuan@unsw.edu.au).

Ying-Chang Liang is with the National Key Laboratory of Wireless Communications, and the Center for Intelligent Networking and Communications (CINC), University of Electronic Science and Technology of China (UESTC), Chengdu 611731, China (e-mail: liangyc@ieee.org).

Rui Zhang is with the School of Science and Engineering, Shenzhen Research Institute of Big Data, The Chinese University of Hong Kong, Shenzhen, Guangdong 518172, China (e-mail: rzhang@cuhk.edu.cn).

These advanced communication paradigms are promising to significantly enhance data throughput and spectral efficiency. However, broadband communication systems face a critical challenge due to time-dispersive channels caused by multi-path propagation, leading to inter-symbol interference (ISI) [4], [5]. Such interference degrades the overall system performance, causing signal distortion which deteriorates the reliability of data transmission.

Numerous methods have been proposed to address the ISI issue, including time-domain and frequency-domain techniques. Specifically, time-domain equalization techniques at the receiver are traditional methods for mitigating ISI, such as linear equalizers [6], [7] and decision feedback equalization (DFE) [8]. Linear equalizers are designed to reverse the effects of the channel dispersion by applying the linear filter, but their complexity increases with longer channel delay spread. DFE improves the equalization performance by incorporating previously detected symbols into the feedback loop, thereby reducing error rates. However, it is more complex to implement and its practical performance is sensitive to error propagation [8]. Precoding techniques, such as linear precoding and Tomlinson–Harashima (TH) precoding, can also be applied at the transmitter for eliminating ISI in the time domain [9], [10]. Their basic ideas are similar to equalization at the receiver, whereas they are implemented at the transmitter side. Besides, time reversal (TR) filters transmit signal with the time reverse of the channel impulse responses (CIR), so that multi-path signals are coherently combined at the receiver, thus effectively reducing ISI [11], [12]. However, in MIMO systems, ISI can only be eliminated asymptotically as the number of the base station (BS) antennas goes to infinity, and the implementation of TR requires rate back-off techniques, which results in a reduction in spectral efficiency [13], [14]. RAKE receivers are commonly used in code-division multiple access (CDMA) systems, by applying multiple delayed matched filters to capture and combine signals from different paths coherently at the receiver [5]. However, due to the use of spread spectrum technology, a much larger bandwidth than that of the transmitted information is required, and their spectral efficiency is limited. Moreover, integrating CDMA in MIMO systems incurs even higher complexity as additional spatial interference needs to be coped with [15]. An ISI suppression method using space time block coding (STBC) or space frequency block coding (SFBC) and statistical pre-filtering (SPF) was proposed in [16] and [17], where SPF

combines transmit beamforming with signal pre-alignment. This approach not only achieves beamforming gain and ISI mitigation with SPF, but also achieves path diversity gain with STBC/SFBC simultaneously. However, the detailed designs provided in [16]–[18] are applicable to wireless channels involving two paths only. Furthermore, in rich multi-path environments, where more than two beams are utilized and orthogonal STBC is applied to mitigate ISI, a rate penalty is incurred due to the coding rate being strictly less than one [16] for a large number of antennas.

On the other hand, frequency-domain equalization is an alternative way to address the ISI issue [19]–[21]. It involves transforming the signal into the frequency domain, applying equalization, and then transforming it back to the time domain. This approach is particularly effective in combating ISI in wideband channels with frequency-domain modulation techniques and can be efficiently implemented using the fast Fourier transform (FFT). In particular, orthogonal frequency division multiplexing (OFDM) stands out among various frequency-domain ISI-mitigation modulation techniques for its robustness and efficiency [5], [22]. By dividing the high-rate data stream into multiple parallel low-rate data streams over different sub-carriers, OFDM converts a frequency-selective channel into multiple frequency-flat channels, thus simplifying equalization while effectively eliminating ISI. However, OFDM also faces several critical issues in practical systems. For instance, the high peak-to-average-power ratio (PAPR) caused by the superposition of multiple sub-carrier signals in the time domain can lead to nonlinear distortion of power amplifiers [23], [24]. Moreover, it suffers from severe out-of-band (OOB) emission that can cause adjacent channel interference [25], and is sensitive to carrier frequency offset (CFO) [26]. More recently, new wideband modulation techniques such as orthogonal time-frequency-space (OTFS) modulation [27]–[29] and orthogonal delay-Doppler division multiplexing (ODDM) modulation [30] have attracted much attention, which perform modulation in the delay-Doppler domain. In addition to overcoming frequency-selective fading of the channel, they can counteract significant Doppler effects that occur in highly mobile environments. However, they also incur high implementation complexity and more signal processing latency.

In contrast to the aforementioned techniques, delay alignment modulation (DAM) was proposed recently as a new means to deal with ISI [31]. It builds upon the novel concepts of *delay pre-compensation* and *path-based beamforming*, which can achieve ISI mitigation and path diversity gain simultaneously. Note that unlike [16], STBC is not required for DAM. In ideal cases, DAM can achieve optimal performance without the need for traditional equalization methods such as channel equalization or multi-carrier transmission. Specifically, by exploiting the high spatial resolution offered by large antenna arrays [32] and leveraging the sparsity of multi-path propagation in mmWave/THz channels [33]–[35], DAM can completely remove the ISI by properly designing symbol delays at the transmitter to compensate for different delays of multi-path components in the channel. Subsequently, by employing path-based beamforming techniques, all multi-

path signal components that reach the receiver simultaneously can be constructively combined. As a result, this technique not only eliminates ISI at the receiver but also enables full utilization of the channel power contributed by all multi-path components. Moreover, the authors in [36] proposed a more general DAM technique, aimed at reducing the channel delay spread when complete elimination of ISI is infeasible or undesirable. Furthermore, the concept of DAM-OFDM was proposed, offering the potential to reduce the cyclic prefix (CP) length and alleviate the high PAPR issue encountered in conventional OFDM. The application of DAM in multi-user communication and wireless systems assisted by intelligent reflecting surfaces (IRSs) was studied in [37]–[39]. In addition, an efficient channel estimation technique for DAM was proposed in [40]. Furthermore, [41] investigated DAM for the more general and practical scenarios with fractional multi-path delays. Integrated sensing and communications (ISAC) based on DAM were investigated in [42]–[45]. In addition, [46] focused on a THz ISAC system that employs active reconfigurable intelligent surfaces (RIS) and DAM, while the secure transmission problem for such a system was later studied in [47]. To further overcome the Doppler effects in the high-mobility communication, delay-Doppler alignment modulation (DDAM) was proposed by leveraging the *delay-Doppler compensation* and *path-based beamforming* [48], which is a generalization of DAM. Compared to OFDM and OTFS, DDAM offers lower PAPR, higher spectral efficiency, and lower complexity at both the transmitter and receiver, especially in scenarios with fewer multi-paths and a large number of information-bearing symbols transmitted per channel coherence block [49]. Additionally, it can be combined with other waveform design techniques to improve their performance, such as DDAM-OFDM and DDAM-OTFS [49], [50].

The aforementioned works have demonstrated the great potential of DAM for spatially sparse channels with large antenna arrays, for enhancing spectral efficiency, reducing PAPR, and simplifying receiver design. However, the previous works on DAM or its extensions have assumed fully digital beamforming, which may incur substantial hardware cost and power consumption since the required number of radio frequency (RF) chains needs to be equal to the number of antennas. To address this issue, significant research endeavors have been devoted to the investigation of hybrid analog/digital beamforming, which greatly reduces the number of RF chains for connecting the digital beamformer and analog beamformer [51]–[53].

Therefore, in this paper, we propose the DAM architecture based on hybrid analog/digital beamforming [54], which aims to achieve DAM performance comparable to that of fully digital beamforming, but with a smaller number of RF chains. This paper thus aims to explore how DAM can be realized based on hybrid analog/digital beamforming, thus providing new practical designs to further reduce the power consumption and hardware cost for implementing DAM. The main contributions of this paper are summarized as follows:

- This paper introduces a new architecture of DAM using hybrid analog/digital beamforming, which includes both

fully connected and partially connected structures. In our preliminary work [54], DAM was considered for the path-based channel model with integer delays. In contrast, this paper further explores DAM based on the more general tap-based channel model with fractional delays [40], [41].

- To reduce the overhead and complexity associated with channel estimation, a new method for implementing DAM via codebook-based beam alignment is proposed. Specifically, the analog beamforming vectors are determined first by searching the discrete Fourier transform (DFT) codebook, which helps in aligning the beams efficiently. After obtaining the analog beamforming matrix, to determine the digital beamforming matrix, only the equivalent channel needs to be estimated, which has a dimension much smaller than the original channel dimension.
- Under the tap-based channel model with fractional delays, where taps within the same cluster may exhibit strong correlation and thus the conventional ISI-zero-forcing (ISI-ZF) beamforming [31] becomes ineffective, DAM-OFDM based on hybrid beamforming is thus proposed. This method aligns each cluster using DAM and then uses OFDM to further address the residual ISI that has much smaller channel spread. This not only leverages the advantage of DAM in reducing delay spread to significantly reduce the number of OFDM sub-carriers or CP overhead, but also takes advantage of OFDM's capability for flexible time-frequency resource allocations.
- The effectiveness of the proposed methods, including hybrid beamforming based DAM, beam alignment based DAM, and hybrid beamforming based DAM-OFDM, is validated through simulations.

The rest of this paper is organized as follows. Section II presents the system model, where both the path-based and tap-based channel models are introduced. The key ideas of DAM based on hybrid beamforming with fully connected and partially connected structures are detailed in Section III. Section IV proposes the beam alignment based DAM to reduce the channel estimation overhead. DAM-OFDM based on hybrid beamforming to overcome the challenges in channels with fractional delays is presented in Section V. Section VI provides the simulation results and Section VII concludes the paper.

Notations: Scalars are denoted by italic letters, and for real numbers x and y , $\lceil x \rceil$ denotes ceiling operations on x , and $\text{mod}(x, y)$ returns the remainder on dividing x by y . Vectors are denoted by boldface lower-case letters, and for a vector \mathbf{x} , $\|\mathbf{x}\|$ denotes its l_2 -norm. Matrices are denoted by boldface upper-case letters. \mathbf{X}^T , \mathbf{X}^* , \mathbf{X}^H , \mathbf{X}^\dagger and $\|\mathbf{X}\|_F$ denote the transpose, conjugate, Hermitian transpose, pseudo-inverse and Frobenius norm of matrix \mathbf{X} , respectively. The block diagonal matrix is denoted by $\text{diag}(\mathbf{x}_1, \mathbf{x}_2, \dots, \mathbf{x}_n)$, where each block is a column vector and its diagonal elements are $\mathbf{x}_i, i = 1, \dots, n$. Sets are denoted by capital calligraphy letters, and for a set \mathcal{X} , $|\mathcal{X}|$ denotes its cardinality. $\mathbb{C}^{M \times N}$ denotes the space of $M \times N$ complex-valued matrices. The imaginary unit of complex numbers is denoted by the symbol j , with $j^2 = -1$. $\mathbb{E}(\cdot)$ and $*$ denote the statistical expectation

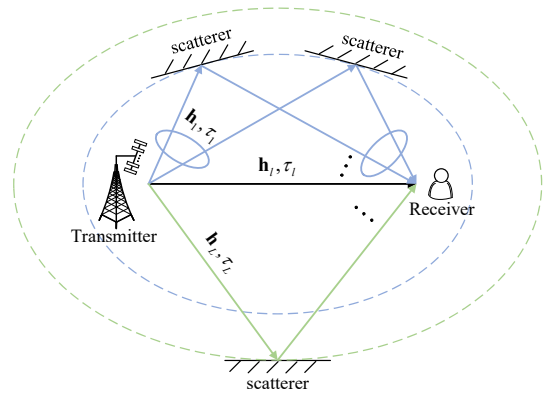


Fig. 1: A MISO spatially sparse mmWave/THz communication system with fractional multi-path delays [41].

and the linear convolution operation, respectively. $\mathcal{CN}(\mu, \sigma^2)$ denotes the distribution of a circularly symmetric complex Gaussian (CSCG) random variable with expected value μ and variance σ^2 , and \sim stands for “distributed as”. $\delta[\cdot]$ denotes the Kronecker delta function.

II. SYSTEM MODEL

As shown in Fig. 1, we consider a spatially sparse wireless communication system, such as mmWave or THz system, in which a base station (BS) equipped with $M_t \gg 1$ antennas engages in communication with a single-antenna user equipment (UE). For cost-effective implementation, the BS has only $M_{\text{RF}} < M_t$ RF chains, and hybrid analog/digital beamforming is applied. We assume a quasi-static block fading environment, where the channel remains constant within each coherent block and may vary across blocks.

Considering the path-based channel model used in the previous work [54], the discrete-time representation of the downlink channel impulse response is

$$\mathbf{h}_{\text{DL}}^H[n] = \sum_{l=1}^L \mathbf{h}_l^H \delta[n - n_l], \quad (1)$$

where L represents the number of temporally resolvable multi-paths, $\mathbf{h}_l \in \mathbb{C}^{M_t \times 1}$ and n_l represent the channel vector and the discretized delay of the l th multi-path, respectively. Let the minimum delay among all L multi-paths be denoted by $n_{\min} \triangleq \min_{1 \leq l \leq L} n_l$, and the maximum delay be denoted by $n_{\max} \triangleq \max_{1 \leq l \leq L} n_l$. Thus, $n_{\text{span}} = n_{\max} - n_{\min}$ represents the normalized channel delay spread. Note that multi-path delays in the channel model of (1) are assumed to be integer multiples of sampling interval T_s . However, the delay of multi-paths may be non-integer multiples of T_s in reality. To generalize our approach and facilitate channel estimation in [40], the tap-based channel model should be considered further. Considering the tap-based channel model, the q th delay tap of the downlink baseband channel can be expressed as [40]

$$\mathbf{h}_{\text{DL}}^H[q] = \sum_{l=1}^L \mathbf{h}_l^H p(qT_s - \tau_l), \quad q = 0, \dots, Q, \quad (2)$$

where $p(t)$ is the pulse shaping function and τ_l represents the physical delay of the l th multi-path. Note that the multi-path

delays τ_l do not have to be integer multiples of T_s . The total number of delay taps is $Q + 1 = \lceil \tau_{UB}/T_s \rceil + 1$, where τ_{UB} is a sufficiently large delay value beyond which no significant power can be received. Due to the sparsity of multi-paths in mmWave/THz communications using large antenna arrays, we usually have $L \ll (Q + 1)$ and $L \ll M_t$ [33]–[35]. In this case, out of the $(Q + 1)$ channel taps, only around L taps have significant power. Because each temporally resolvable multi-path in (1) and (2) may comprise multiple sub-paths with the same delay but distinct angles of departure (AoDs), \mathbf{h}_l can be further expressed as [31]

$$\mathbf{h}_l = \alpha_l \sum_{i=1}^{\mu_l} v_{li} \mathbf{a}_t(\theta_{li}), \quad (3)$$

where α_l represents the complex-valued path gain of the l th multi-path, μ_l represents the number of sub-paths within the l th multi-path, $v_{li} = \sqrt{\varsigma_{li}} e^{j\phi_{li}}$ represents the complex coefficient of the i th sub-path of the l th multi-path, where ϕ_{li} denotes the phase of the i th sub-path, and ς_{li} represents the power allocation for the i th sub-path and satisfies the condition $\sum_{i=1}^{\mu_l} \varsigma_{li} = 1$ to ensure the power is normalized, and θ_{li} denotes the AoD of the i th sub-path of the l th multi-path, while $\mathbf{a}_t(\theta_{li}) \in \mathbb{C}^{M_t \times 1}$ denotes the corresponding transmit array response vector. For a basic uniform linear array (ULA), $\mathbf{a}_t(\theta_{li})$ is given by

$$\mathbf{a}_t(\theta_{li}) = \left[1, e^{-j\frac{2\pi d}{\lambda} \sin(\theta_{li})}, \dots, e^{-j\frac{2\pi(M_t-1)d}{\lambda} \sin(\theta_{li})} \right]^T, \quad (4)$$

where λ denotes the signal wavelength and d denotes the inter-element spacing of the ULA.

Let $\mathbf{x}[n] \in \mathbb{C}^{M_t \times 1}$ denote the discrete-time representation of the signals transmitted by the BS. Based on the path-based channel model in (1), the received signal at UE is

$$y[n] = \mathbf{h}_{DL}^H[n] * \mathbf{x}[n] + z[n] = \sum_{l=1}^L \mathbf{h}_l^H \mathbf{x}[n - n_l] + z[n], \quad (5)$$

where $z[n] \sim \mathcal{CN}(0, \sigma^2)$ represents the additive white Gaussian noise (AWGN). Similarly, based on the tap-based channel model, the received signal can be expressed as

$$y[n] = \sum_{q=0}^Q \mathbf{h}_{DL}^H[q] \mathbf{x}[n - q] + z[n]. \quad (6)$$

It can be seen from both (5) and (6) that in a multipath propagation environment, the received signal is a superposition of the transmitted signal with different delays, which can cause ISI. In [31], a novel technique known as DAM was introduced to address the issue of ISI based on *delay pre-compensation* and *path-based beamforming*, obviating the need for conventional methods such as channel equalization or multi-carrier transmission. Yet, the DAM technique presented there assumes the fully digital beamforming at the BS, which cannot be applied for the considered system with fewer RF chains than the number of antennas. In the following, we propose the hybrid analog/digital beamforming based DAM technique for spatially sparse communication systems.

III. DAM WITH HYBRID BEAMFORMING

The transmitter architecture of the proposed DAM system, utilizing hybrid analog/digital beamforming with the fully connected structure, is illustrated in Fig. 2a. This section will consider the implementation of DAM with hybrid beamforming based on path-based and tap-based channel models.

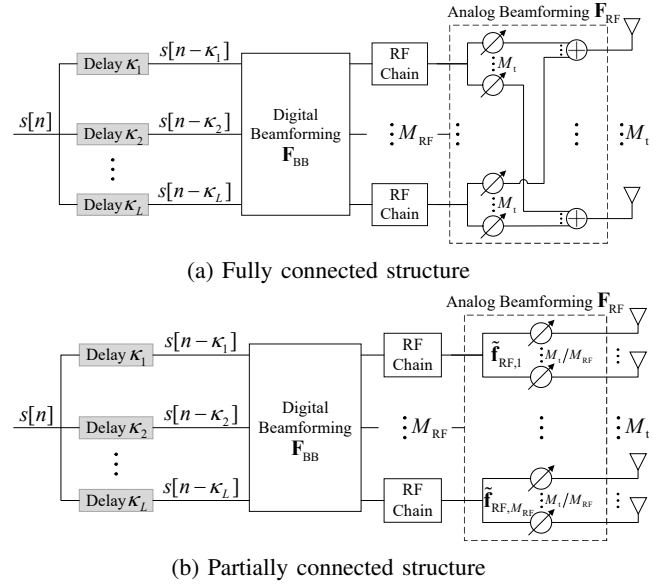


Fig. 2: Transmitter architecture for DAM based on hybrid beamforming with fully connected structure and partially connected structure.

A. Path-based DAM with Hybrid Beamforming

Through *delay pre-compensation* and *path-based beamforming*, the transmitted signal for DAM with hybrid beamforming can be expressed as

$$\mathbf{x}[n] = \mathbf{F}_{RF} \sum_{l=1}^L \mathbf{f}_{BB,l} s[n - \kappa_l], \quad (7)$$

where $\mathbf{F}_{RF} \in \mathbb{C}^{M_t \times M_{RF}}$ denotes the analog beamforming matrix with unit modulus for each of its element, i.e., $|(\mathbf{F}_{RF})_{i,j}| = 1, \forall i, j$, $\mathbf{F}_{BB} \in \mathbb{C}^{M_{RF} \times L}$ denotes the digital baseband beamforming matrix that includes $\mathbf{f}_{BB,l} \in \mathbb{C}^{M_{RF} \times 1}$ for its l th column, $s[n]$ is the independent and identically distributed (i.i.d.) information-bearing symbols satisfying the normalized power requirement $\mathbb{E}[|s[n]|^2] = 1$, and $\kappa_l \geq 0$ denotes the intentionally introduced delay with $\kappa_l \neq \kappa_{l'}, \forall l \neq l'$, aiming to compensate for the delay n_l of the l th channel path.

The power of the transmitted signal $\mathbf{x}[n]$ is

$$\begin{aligned} \mathbb{E}[\|\mathbf{x}[n]\|^2] &= \sum_{l=1}^L \mathbb{E}[\|\mathbf{F}_{RF} \mathbf{f}_{BB,l} s[n - \kappa_l]\|^2] \\ &= \sum_{l=1}^L \|\mathbf{F}_{RF} \mathbf{f}_{BB,l}\|^2 = \|\mathbf{F}_{RF} \mathbf{F}_{BB}\|_F^2 \leq P, \end{aligned} \quad (8)$$

where P represents the available transmit power. By substituting (7) into (5), the received signal of DAM with hybrid analog/digital beamforming is

$$\begin{aligned} y[n] &= \sum_{l=1}^L \mathbf{h}_l^H \mathbf{F}_{RF} \mathbf{f}_{BB,l} s[n - \kappa_l - n_l] + \\ &\quad \sum_{l=1}^L \sum_{l' \neq l} \mathbf{h}_l^H \mathbf{F}_{RF} \mathbf{f}_{BB,l'} s[n - \kappa_{l'} - n_l] + z[n]. \end{aligned} \quad (9)$$

According to the principle of DAM [31], the introduced delay

κ_l is set to $\kappa_l = n_{\max} - n_l \geq 0, \forall l$. Thus, we have

$$y[n] = \left(\sum_{l=1}^L \mathbf{h}_l^H \mathbf{F}_{\text{RF}} \mathbf{f}_{\text{BB},l} \right) s[n - n_{\max}] + \sum_{l=1}^L \sum_{l' \neq l}^L \mathbf{h}_l^H \mathbf{F}_{\text{RF}} \mathbf{f}_{\text{BB},l'} s[n - n_{\max} + n_{l'} - n_l] + z[n]. \quad (10)$$

Observing (10), it becomes apparent that the first term contributes to the desired signal if the receiver is locked to the delay n_{\max} , whereas the second term represents the ISI. Furthermore, the ISI can be eliminated by jointly designing \mathbf{F}_{RF} and \mathbf{F}_{BB} to satisfy

$$\mathbf{h}_l^H \mathbf{F}_{\text{RF}} \mathbf{f}_{\text{BB},l'} = 0, \forall l' \neq l. \quad (11)$$

Subsequently, the received signal in (10) simplifies to

$$y[n] = \left(\sum_{l=1}^L \mathbf{h}_l^H \mathbf{F}_{\text{RF}} \mathbf{f}_{\text{BB},l} \right) s[n - n_{\max}] + z[n]. \quad (12)$$

It can be seen from (12) that if condition in (11) is satisfied, the ISI can be eliminated perfectly and the received signal becomes a symbol sequence with a single delay n_{\max} and multiplied by the gains with L multi-path contributions. The method in (11) is known as ISI-ZF beamforming. In this case, the SNR is

$$\gamma = \frac{1}{\sigma^2} \left| \sum_{l=1}^L \mathbf{h}_l^H \mathbf{F}_{\text{RF}} \mathbf{f}_{\text{BB},l} \right|^2. \quad (13)$$

As a result, the analog and digital beamforming matrices \mathbf{F}_{RF} and \mathbf{F}_{BB} need to be jointly designed to maximize the spectral efficiency of path-based DAM with the ISI-ZF constraint in (11). The problem can be stated as

$$\max_{\mathbf{F}_{\text{RF}}, \mathbf{F}_{\text{BB}}} \log_2 \left(1 + \frac{1}{\sigma^2} \left| \sum_{l=1}^L \mathbf{h}_l^H \mathbf{F}_{\text{RF}} \mathbf{f}_{\text{BB},l} \right|^2 \right) \quad (14)$$

$$\text{s.t. } \mathbf{h}_l^H \mathbf{F}_{\text{RF}} \mathbf{f}_{\text{BB},l'} = 0, \forall l' \neq l,$$

$$\left| (\mathbf{F}_{\text{RF}})_{i,j} \right| = 1, \forall i, j, \|\mathbf{F}_{\text{RF}} \mathbf{F}_{\text{BB}}\|_F^2 \leq P.$$

Apparently, the spectral efficiency can be maximized by maximizing the SNR in (13). By discarding the constant term, the problem in (14) can be equivalently stated as

$$\max_{\mathbf{F}_{\text{RF}}, \mathbf{F}_{\text{BB}}} \left| \sum_{l=1}^L \mathbf{h}_l^H \mathbf{F}_{\text{RF}} \mathbf{f}_{\text{BB},l} \right|^2 \quad (15)$$

$$\text{s.t. } \mathbf{h}_l^H \mathbf{F}_{\text{RF}} \mathbf{f}_{\text{BB},l'} = 0, \forall l' \neq l,$$

$$\left| (\mathbf{F}_{\text{RF}})_{i,j} \right| = 1, \forall i, j, \|\mathbf{F}_{\text{RF}} \mathbf{F}_{\text{BB}}\|_F^2 \leq P.$$

Directly solving the optimization problem (15) is difficult, since it is non-convex and the analog and digital beamforming vectors are closely coupled. By following the similar idea of hybrid beamforming optimization as [52], we may first determine the optimal solution for fully digital beamforming design, and then find the hybrid analog/digital beamforming matrices to closely approximate the optimal fully digital beamforming. Specifically, by letting $\mathbf{F}_{\text{RF}} \mathbf{f}_{\text{BB},l} = \mathbf{f}_l, \forall l$, a new beamforming problem for DAM can be formulated as

$$\max_{\{\mathbf{f}_l\}_{l=1}^L} \left| \sum_{l=1}^L \mathbf{h}_l^H \mathbf{f}_l \right|^2 \quad (16)$$

$$\text{s.t. } \mathbf{h}_l^H \mathbf{f}_{l'} = 0, \forall l' \neq l, \sum_{l=1}^L \|\mathbf{f}_l\|^2 \leq P.$$

Note that problem (16) corresponds to ISI-ZF for DAM with fully digital beamforming, whose optimal solution $\{\mathbf{f}_l^{\text{opt}}\}_{l=1}^L$ has been obtained in closed-form in [31].

In order to achieve the same performance as fully digital beamforming based DAM, \mathbf{F}_{RF} and \mathbf{F}_{BB} should be jointly designed to satisfy

$$\mathbf{F}_{\text{RF}} \mathbf{f}_{\text{BB},l} = \mathbf{f}_l^{\text{opt}}, \forall l. \quad (17)$$

By letting $\mathbf{F}_{\text{opt}} = [\mathbf{f}_1^{\text{opt}}, \mathbf{f}_2^{\text{opt}}, \dots, \mathbf{f}_L^{\text{opt}}] \in \mathbb{C}^{M_t \times L}$, (17) can be compactly expressed as: $\mathbf{F}_{\text{RF}} \mathbf{F}_{\text{BB}} = \mathbf{F}_{\text{opt}}$. Note that the rank of \mathbf{F}_{opt} is L when the vectors $\mathbf{h}_l, \forall l$ are linearly independent [54]. On the other hand, the rank of $\mathbf{F}_{\text{RF}} \mathbf{F}_{\text{BB}}$ is no greater than M_{RF} . This indicates that for (17) to hold, one necessary condition is $M_{\text{RF}} \geq L$ [55], [56]. Furthermore, it was revealed in [56] that when $M_{\text{RF}} \geq 2L$, \mathbf{F}_{RF} and \mathbf{F}_{BB} can be found to satisfy $\mathbf{F}_{\text{RF}} \mathbf{F}_{\text{BB}} = \mathbf{F}_{\text{opt}}$ exactly, indicating that hybrid beamforming based DAM can fully realize the performance of fully digital beamforming when $M_{\text{RF}} \geq 2L$.

With the optimal ISI-ZF beamforming matrix \mathbf{F}_{opt} for fully digital beamforming obtained, hybrid beamforming for DAM can be designed by considering the optimization problem as

$$\min_{\mathbf{F}_{\text{RF}}, \mathbf{F}_{\text{BB}}} \|\mathbf{F}_{\text{opt}} - \mathbf{F}_{\text{RF}} \mathbf{F}_{\text{BB}}\|_F \quad (18)$$

$$\text{s.t. } \left| (\mathbf{F}_{\text{RF}})_{i,j} \right| = 1, \forall i, j, \|\mathbf{F}_{\text{RF}} \mathbf{F}_{\text{BB}}\|_F^2 = P.$$

Our previous work in [54] has proposed a solution for this problem, which transforms it into the following optimization problem

$$\min_{\mathbf{F}_{\text{RF}}, \mathbf{F}_{\text{BB}}} \|\mathbf{F}_{\text{opt}} - \mathbf{F}_{\text{RF}} \mathbf{F}_{\text{BB}}\|_F \quad (19)$$

$$\text{s.t. } \mathbf{f}_{\text{RF},j} \in \mathbf{a}_t(\theta_{li}), \forall l, i, j, \|\mathbf{F}_{\text{RF}} \mathbf{F}_{\text{BB}}\|_F^2 = P.$$

This problem can be solved with the orthogonal matching pursuit (OMP) algorithm in [52], which is omitted here for brevity.

Note that the above optimization problem considers a hybrid analog/digital beamforming design based on the fully connected structure as shown in Fig. 2a. In the fully connected hybrid beamforming structure, each RF chain is connected to all the antenna elements. This structure is highly flexible, capable of achieving finer beam control and higher array gain, but it brings higher complexity and power consumption, since the total number of analog phase shifters required is $M_{\text{RF}} M_t$. For further cost and power savings, hybrid beamforming based on the partially connected structure can be considered, as shown in Fig. 2b. In the partially connected structure, each RF chain is connected to only a subset of the antenna elements, adding another constraint to the analog beamforming matrix $\bar{\mathbf{F}}_{\text{RF}}$, i.e., only a portion of the elements of $\bar{\mathbf{F}}_{\text{RF}}$ can be designed, with the remaining elements being zero. Specifically, assuming that $M = M_t / M_{\text{RF}}$ antennas are connected to each RF chain, the analog beamforming matrix can be expressed as $\bar{\mathbf{F}}_{\text{RF}} = \text{diag}(\bar{\mathbf{f}}_{\text{RF},1}, \bar{\mathbf{f}}_{\text{RF},2}, \dots, \bar{\mathbf{f}}_{\text{RF},M_{\text{RF}}})$, where $\bar{\mathbf{f}}_{\text{RF},t} \in \mathbb{C}^{M \times 1}$ denotes the beamforming vector for the t th RF chain and M is assumed to be an integer for notational convenience. As a result, the optimization problem for hybrid beamforming based

DAM with the partially connected structure is given by

$$\begin{aligned} \min_{\tilde{\mathbf{F}}_{\text{RF}}, \mathbf{F}_{\text{BB}}} & \left\| \mathbf{F}_{\text{opt}} - \tilde{\mathbf{F}}_{\text{RF}} \mathbf{F}_{\text{BB}} \right\|_F \\ \text{s.t.} & \tilde{\mathbf{f}}_{\text{RF},t} \in \mathbf{a}_t(\theta_{li})_{1+(t-1)M:tM}, \forall t, l, i, \\ & \left\| \tilde{\mathbf{F}}_{\text{RF}} \mathbf{F}_{\text{BB}} \right\|_F^2 = P. \end{aligned} \quad (20)$$

According to the method in [51], the power constraint in (20) can be temporally removed. So this problem can be decoupled into multiple single-objective optimization problems as

$$\begin{aligned} \min_{\tilde{\mathbf{f}}_{\text{RF},t}, (\mathbf{F}_{\text{BB}})_{t,:}} & \left\| (\mathbf{F}_{\text{opt}})_{1+(t-1)M:tM,:} - \tilde{\mathbf{f}}_{\text{RF},t} (\mathbf{F}_{\text{BB}})_{t,:} \right\|_F, \forall t, \\ \text{s.t.} & \tilde{\mathbf{f}}_{\text{RF},t} \in \mathbf{a}_t(\theta_{li})_{1+(t-1)M:tM}, \forall t, l, i. \end{aligned} \quad (21)$$

These problem can also be solved using the OMP algorithm in [52], and the solutions are denoted by $\tilde{\mathbf{F}}_{\text{RF}}^{\text{opt}}$ and $\mathbf{F}_{\text{BB}}^{\text{opt}}$. Finally, to satisfy the power constraint in (20), $\mathbf{F}_{\text{BB}}^{\text{opt}}$ needs to be normalized by a factor of $\sqrt{P}/\|\tilde{\mathbf{F}}_{\text{RF}}^{\text{opt}} \mathbf{F}_{\text{BB}}^{\text{opt}}\|_F$.

Because of the unit modulus constraint imposed on the analog beamforming matrix, the performance of hybrid beamforming based on the fully connected structure may be different from the optimal fully digital beamforming when $M_{\text{RF}} < 2L$, and the performance based on partially connected structures is even worse. In other words, with the aforementioned hybrid analog/digital beamforming design, there is no guarantee that the ISI-ZF constraint in (11) can be satisfied. This implies that for the purpose of evaluating the resulting performance of DAM based on hybrid analog/digital beamforming, the residual ISI needs to be considered.

To this end, the same delay components in (10) should be grouped together [31]. Specifically, let $\mathcal{L} \triangleq \{l : l = 1, \dots, L\}$ denote the set of all multi-paths, and $\mathcal{L}_l \triangleq \mathcal{L} \setminus l$ represent the subset of set \mathcal{L} by removing the l th path from it. Furthermore, let the delay difference between l' and l be denoted by $\Delta_{l',l} \triangleq n_{l'} - n_l$. Then, for $\forall l \neq l'$, $\Delta_{l',l} \in \{\pm 1, \dots, \pm n_{\text{span}}\}$. Thus, (10) can be equivalently expressed as

$$\begin{aligned} y[n] = & \left(\sum_{l=1}^L \mathbf{h}_l^H \mathbf{F}_{\text{RF}} \mathbf{f}_{\text{BB},l} \right) s[n - n_{\text{max}}] + \\ & \sum_{l=1}^L \sum_{l' \neq l}^L \mathbf{h}_l^H \mathbf{F}_{\text{RF}} \mathbf{f}_{\text{BB},l'} s[n - n_{\text{max}} + \Delta_{l',l}] + z[n]. \end{aligned} \quad (22)$$

The terms with the same delay difference in (22) correspond to the same symbols, which need to be grouped. For each delay difference $i \in \{\pm 1, \dots, \pm n_{\text{span}}\}$, the effective channel can be defined as

$$\mathbf{g}_{l'}^H[i] \triangleq \begin{cases} \mathbf{h}_l^H, & \text{if } \exists l \in \mathcal{L}_{l'}, \text{ s.t. } n_{l'} - n_l = i, \\ \mathbf{0}, & \text{otherwise.} \end{cases} \quad (23)$$

Therefore, (22) can be expressed equivalently as

$$\begin{aligned} y[n] = & \left(\sum_{l=1}^L \mathbf{h}_l^H \mathbf{F}_{\text{RF}} \mathbf{f}_{\text{BB},l} \right) s[n - n_{\text{max}}] + \\ & \sum_{i=-n_{\text{span}}, i \neq 0}^{n_{\text{span}}} \left(\sum_{l'=1}^L \mathbf{g}_{l'}^H[i] \mathbf{F}_{\text{RF}} \mathbf{f}_{\text{BB},l'} \right) s[n - n_{\text{max}} + i] + \\ & z[n]. \end{aligned} \quad (24)$$

Then, the signal-to-interference-plus-noise ratio (SINR) of

DAM with hybrid beamforming is

$$\gamma = \frac{\left| \sum_{l=1}^L \mathbf{h}_l^H \mathbf{F}_{\text{RF}} \mathbf{f}_{\text{BB},l} \right|^2}{\sum_{i=-n_{\text{span}}, i \neq 0}^{n_{\text{span}}} \left| \sum_{l'=1}^L \mathbf{g}_{l'}^H[i] \mathbf{F}_{\text{RF}} \mathbf{f}_{\text{BB},l'} \right|^2 + \sigma^2}. \quad (25)$$

B. Tap-based DAM with Hybrid Beamforming

Considering the more general tap-based channel model, the multi-path delays τ_l in (2) may be non-integer multiples of T_s . This will lead to strong channel correlation on adjacent taps, so aligning all taps with relatively strong channel strengths to a single tap would make ISI-ZF beamforming unachievable.

To address this issue, the relatively strong taps are grouped into L' clusters, and the adjacent taps are grouped into one cluster, which is considered to have strong channel correlations within each cluster. Specifically, we need to find out the relatively weak taps with power smaller than $C \max_q \|\mathbf{h}_{\text{DL}}[q]\|^2$, where $C < 1$ is a certain threshold. They are considered insignificant and set to zero. Then, the remaining non-zero taps are grouped based on their adjacency, i.e., consecutive non-zero taps are grouped into a single cluster, with the assumption that taps within the same cluster exhibit strong channel correlations. Consequently, the strongest tap within each cluster can be aligned to the same tap through *delay pre-compensation*, and finally, minimum mean-square error (MMSE) beamforming can be applied. Similar to (7), the transmitted signal is

$$\mathbf{x}[n] = \mathbf{F}_{\text{RF}} \sum_{l=1}^{L'} \mathbf{f}_{\text{BB},l} s[n - \kappa_l], \quad (26)$$

where $L' \leq L$ denotes the number of channel taps that need to be aligned. By substituting (26) to (6), the received signal can be expressed as

$$y[n] = \sum_{q=0}^Q \mathbf{h}_{\text{DL}}^H[q] \sum_{l=1}^{L'} \mathbf{F}_{\text{RF}} \mathbf{f}_{\text{BB},l} s[n - \kappa_l - q] + z[n]. \quad (27)$$

By letting $\mathbf{F}_{\text{RF}} \mathbf{f}_{\text{BB},l} = \mathbf{f}_l, \forall l$ to determine the optimal solution for fully digital beamforming design first, $y[n]$ can be further expressed as

$$y[n] = \sum_{q=0}^Q \sum_{l=1}^{L'} \mathbf{h}_{\text{DL}}^H[q] \mathbf{f}_l s[n - \kappa_l - q] + z[n]. \quad (28)$$

Let $q_l, l = 1, \dots, L'$ be the strongest tap within the l th cluster and align taps $\{q_l\}_{l=1}^{L'}$ to the tap $q_{\text{max}} = \max_{1 \leq l \leq L'} q_l$, i.e., let $\kappa_l = q_{\text{max}} - q_l$, (28) can be further expressed as

$$\begin{aligned} y[n] = & \left(\sum_{l=1}^{L'} \mathbf{h}_{\text{DL}}^H[q_l] \mathbf{f}_l \right) s[n - q_{\text{max}}] \\ & + \sum_{l=1}^{L'} \sum_{q \neq q_l}^Q \mathbf{h}_{\text{DL}}^H[q] \mathbf{f}_l s[n - q_{\text{max}} + q_l - q] + z[n]. \end{aligned} \quad (29)$$

Observing (29), it becomes apparent that the first term contributes to the desired signal if the receiver is locked to the tap q_{max} , whereas the second term represents the ISI. Since the terms with the same delay correspond to the same symbols, which need to be grouped, we define the effective channel as

$$\mathbf{g}_l^H[i] = \begin{cases} \mathbf{h}_{\text{DL}}^H[q], & \text{if } \exists l \in \{1, \dots, L'\}, \text{ s.t. } q_l - q = i, \\ \mathbf{0}, & \text{otherwise,} \end{cases} \quad (30)$$

where $i \in \{\pm 1, \dots, \pm Q\}$. Thus, (29) can be further expressed as

$$y[n] = \left(\sum_{l=1}^{L'} \mathbf{h}_{\text{DL}}^H[q_l] \mathbf{f}_l \right) s[n - q_{\text{max}}] + \sum_{i=-Q, i \neq 0}^Q \left(\sum_{l=1}^{L'} \mathbf{g}_l^H[i] \mathbf{f}_l \right) s[n - q_{\text{max}} + i] + z[n]. \quad (31)$$

The resulting SINR is

$$\gamma = \frac{\left| \sum_{l=1}^{L'} \mathbf{h}_{\text{DL}}^H[q_l] \mathbf{f}_l \right|^2}{\sum_{i=-Q, i \neq 0}^Q \left| \sum_{l=1}^{L'} \mathbf{g}_l^H[i] \mathbf{f}_l \right|^2 + \sigma^2} = \frac{\bar{\mathbf{f}}^H \bar{\mathbf{h}}_{\text{DL}} \bar{\mathbf{h}}_{\text{DL}}^H \bar{\mathbf{f}}}{\bar{\mathbf{f}}^H \left(\sum_{i=-Q, i \neq 0}^Q \bar{\mathbf{g}}[i] \bar{\mathbf{g}}^H[i] + \sigma^2 \mathbf{I} / \|\bar{\mathbf{f}}\|^2 \right) \bar{\mathbf{f}}}, \quad (32)$$

where $\bar{\mathbf{h}}_{\text{DL}} = [\mathbf{h}_{\text{DL}}^T[q_1], \dots, \mathbf{h}_{\text{DL}}^T[q_{L'}]]^T \in \mathbb{C}^{M_t L' \times 1}$, $\bar{\mathbf{f}} = [\mathbf{f}_1^T, \dots, \mathbf{f}_{L'}^T]^T \in \mathbb{C}^{M_t L' \times 1}$, and $\bar{\mathbf{g}}[i] = [\mathbf{g}_1^T[i], \dots, \mathbf{g}_{L'}^T[i]]^T \in \mathbb{C}^{M_t L' \times 1}$. To maximize the spectral efficiency of tap-based DAM, SINR in (32) should be maximized and thus the digital beamforming vector should be designed as

$$\bar{\mathbf{f}}^{\text{MMSE}} = \sqrt{P} \mathbf{C}^{-1} \bar{\mathbf{h}}_{\text{DL}} / \|\mathbf{C}^{-1} \bar{\mathbf{h}}_{\text{DL}}\|. \quad (33)$$

where $\mathbf{C} \triangleq \sum_{i=-Q, i \neq 0}^Q \bar{\mathbf{g}}[i] \bar{\mathbf{g}}^H[i] + \sigma^2 / P \mathbf{I}$, with $\|\bar{\mathbf{f}}\|^2 = P$. Thus, the optimal fully digital beamforming matrix based on MMSE can be obtained, noted by $\mathbf{F}_{\text{opt}}^{\text{MMSE}}$. Exploiting the idea of hybrid beamforming in the previous subsection, substituting $\mathbf{F}_{\text{opt}}^{\text{MMSE}}$ into the optimization problem (19) or (21) and solving it, the hybrid analog/digital beamforming design can be obtained.

IV. BEAM ALIGNMENT BASED DAM

For the aforementioned DAM technique based on fully digital or hybrid analog/digital beamforming, it is necessary to estimate the channel state information (CSI). However, the estimation overhead and complexity of the complete CSI matrix become impractical as the number of antenna elements increases. Besides, for massive MIMO systems with DAM, significant computational overhead is incurred. In the following, we propose a codebook-based beam alignment DAM technique to reduce the complexity of channel estimation.

Based on the transmitter architecture in Fig. 2a, achieving beam alignment based DAM involves two stages: codebook-based analog beamforming and digital beamforming.

A. Codebook-based Analog Beamforming Design

To reduce the cost of channel estimation, codebook-based analog beamforming can be used to align the most dominant channel taps. Commonly used equivalent DFT codebook [57] is given by

$$\mathcal{F}_{\text{DFT}} = \left\{ \mathbf{a}_t(\hat{\theta}) : \hat{\theta} \in \Theta \right\}, \quad (34)$$

$$\Theta = \left\{ \hat{\theta} : (1 + \sin(\hat{\theta}))/2 = \frac{m_t - 1}{M_t}, m_t \in [1, M_t] \right\}. \quad (35)$$

Based on the transmitter structure shown in Fig. 2a, to initially determine the analog beamforming matrix \mathbf{F}_{RF} , the

l th column of the analog beamforming matrix denoted by $\mathbf{f}_{\text{RF},l} \in \mathbb{C}^{M_t \times 1}$ is selected from the DFT codebook in (34), and the digital beamforming matrix \mathbf{F}_{BB} is set as the identity matrix, i.e., $\mathbf{f}_{\text{RF},l} \in \mathcal{F}_{\text{DFT}}$, $\mathbf{F}_{\text{BB}} = \mathbf{I}_{M_{\text{RF}}}$. Note that *delay pre-compensation* is neither required nor achievable at this stage due to the lack of CSI. So one difference from Fig. 2a is that in this stage, instead of digital beamforming the signal with *delay pre-compensation*, we directly input the pilot sequences for digital beamforming. Thus, the transmitted signal can be expressed as

$$\mathbf{x}[n] = \mathbf{F}_{\text{RF}} \mathbf{F}_{\text{BB}} \mathbf{P} \mathbf{m}[n] = \mathbf{F}_{\text{RF}} \mathbf{P} \mathbf{m}[n] = \sum_{l=1}^{M_{\text{RF}}} \sqrt{p_l} \mathbf{f}_{\text{RF},l} m_l[n], \quad (36)$$

where $\mathbf{m}[n] = [m_1[n], m_2[n], \dots, m_{M_{\text{RF}}}[n]]^T \in \mathbb{C}^{M_{\text{RF}} \times 1}$ includes M_{RF} pilot sequences, and $\mathbf{P} = \text{diag}(\sqrt{p_1}, \sqrt{p_2}, \dots, \sqrt{p_{M_{\text{RF}}}}) \in \mathbb{C}^{M_{\text{RF}} \times M_{\text{RF}}}$ is the power allocation matrix with p_l , $\forall l = 1, \dots, M_{\text{RF}}$ denoting the transmit power allocated to the l th sequence. Note that $m_l[n]$ is independent for different l and n , and it has the normalized power, i.e., $\mathbb{E}[|m_l[n]|^2] = 1$. The transmit power of (36) is

$$\mathbb{E}[\|\mathbf{x}[n]\|^2] = \sum_{l=1}^{M_{\text{RF}}} \mathbb{E}[\|\sqrt{p_l} \mathbf{f}_{\text{RF},l} m_l[n]\|^2] = \sum_{l=1}^{M_{\text{RF}}} p_l \|\mathbf{f}_{\text{RF},l}\|^2 \leq P. \quad (37)$$

Assuming an equal allocation of transmit power, i.e., $p_l = \bar{p}$, $\forall l$, we can further obtain

$$\mathbb{E}[\|\mathbf{x}[n]\|^2] = \bar{p} \sum_{l=1}^{M_{\text{RF}}} \|\mathbf{f}_{\text{RF},l}\|^2 = \bar{p} \|\mathbf{F}_{\text{RF}}\|_F^2 \leq P. \quad (38)$$

From this, it can be derived that $\bar{p} \leq P / \|\mathbf{F}_{\text{RF}}\|_F^2$.

Note that $m_l[n]$, $\forall l \in [1, M_{\text{RF}}]$ can be a pseudo-random sequence with period T_m , e.g., Zadoff-Chu (ZC) sequence, which has good autocorrelation and cross-correlation properties. These properties help the receiver to separate different beams in the codebook that are being transmitted simultaneously. Let the autocorrelation and cross-correlation of the sequence be

$$R_{m_l}[n] = \begin{cases} \frac{1}{T_m} \sum_{i=0}^{T_m-1} m_l[i] m_l^*[i] = R_{\text{max}}, n = 0, \\ \frac{1}{T_m} \sum_{i=0}^{T_m-1} m_l[i] m_l^*[i-n] \approx 0, n \in [1, T_m-1], \end{cases} \quad (39)$$

$$R_{m_l, m_{l'}}[n] = \frac{1}{T_m} \sum_{i=0}^{T_m-1} m_l[i] m_{l'}^*[i-n] \approx 0, l \neq l'. \quad (40)$$

It can be inferred from (36) that since there are M_{RF} RF chains, the transmitter is able to search M_{RF} beams in the codebook simultaneously for each transmission. And there are a total of M_t beams in the codebook, so the transmitter needs to transmit $\lceil M_t / M_{\text{RF}} \rceil$ times. As a result, the transmit signal for the t th transmission can be expressed as

$$\mathbf{x}_t[n] = \sqrt{\bar{p}} \sum_{l=1}^{M_{\text{RF}}} \mathbf{f}_{\text{RF},t,l} m_l[n], t \in [1, \lceil M_t / M_{\text{RF}} \rceil]. \quad (41)$$

By substituting (41) to (6), the received signal during the beam searching phase can be expressed as

$$y_t[n] = \sum_{q=0}^Q \mathbf{h}_{\text{DL}}^H[q] \mathbf{x}_t[n-q] + z_t[n] = \sqrt{\bar{p}} \sum_{q=0}^Q \sum_{l=1}^{M_{\text{RF}}} \mathbf{h}_{\text{DL}}^H[q] \mathbf{f}_{\text{RF},t,l} m_l[n-q] + z_t[n]. \quad (42)$$

Because of the cross-correlation properties of pilot sequences in (40), the M_{RF} pilot sequences transmitted from the BS can be approximately separated at the UE by passing the received signal in (42) through a bank of matched filters where the l th filter has impulse response $m_l^*[i-n]$. Thus, it can be obtained that

$$\begin{aligned}
y_{t,l}[n] &= \frac{1}{T_m} \sum_{i=Q}^{Q+T_m-1} y_t[i] m_l^*[i-n] \\
&= \frac{\sqrt{\bar{p}}}{T_m} \sum_{i=Q}^{Q+T_m-1} \sum_{q=0}^Q \sum_{\nu=1}^{M_{\text{RF}}} \mathbf{h}_{\text{DL}}^H[q] \mathbf{f}_{\text{RF},t,\nu} m_{\nu}[i-q] m_l^*[i-n] \\
&\quad + \frac{1}{T_m} \sum_{i=Q}^{Q+T_m-1} z_t[i] m_l^*[i-n] \\
&= \frac{\sqrt{\bar{p}}}{T_m} \sum_{q=0}^Q \sum_{\nu=1}^{M_{\text{RF}}} \mathbf{h}_{\text{DL}}^H[q] \mathbf{f}_{\text{RF},t,\nu} \sum_{i=Q}^{Q+T_m-1} m_{\nu}[i-q] m_l^*[i-n] \\
&\quad + z_t^c[n] \\
&= \sqrt{\bar{p}} \sum_{q=0}^Q \sum_{\nu=1}^{M_{\text{RF}}} \mathbf{h}_{\text{DL}}^H[q] \mathbf{f}_{\text{RF},t,\nu} R_{m_{\nu},m_l}[n-q] + z_t^c[n], \\
n &\in [0, T_m - 1].
\end{aligned} \tag{43}$$

Note that the good cross-correlation properties of sequence $m_l[n], \forall l \in [1, M_{\text{RF}}]$ are based on a complete period T_m . Therefore, in (43), when performing the correlation operation, the range of i is considered to be $[Q, Q + T_m - 1]$, implying that $0 \leq i - q \leq Q + T_m - 1$. Since the period of $R_{m_l, m_{\nu}}[n]$ is T_m , it follows that the period of $y_{t,l}[n]$ is also T_m , so we take the range of n in (43) to be $[0, T_m - 1]$. To ensure that the correlation operation at the receiver is based on a complete period, the transmitter should send the pilot sequences periodically. Assuming that the length of the transmitted sequence in (41) is aT_m , since the index of $m_{\nu}[i-q]$ in (43) is in the range of $0 \leq i - q \leq Q + T_m - 1$, it should satisfy $aT_m - 1 \geq Q + T_m - 1$. Therefore, it is necessary to transmit at least $a = Q/T_m + 1$ periods of the pilot sequences, so that $aT_m \geq Q + T_m$, where T_m needs to be large enough to ensure good cross-correlation properties of the pilot sequences. Note that, when choosing the period of pilot sequences, there is a tradeoff between maintaining good cross-correlation properties and avoiding a significant increase in beam search time.

With (40), (43) can be further simplified as

$$y_{t,l}[n] \approx \sqrt{\bar{p}} \sum_{q=0}^Q \mathbf{h}_{\text{DL}}^H[q] \mathbf{f}_{\text{RF},t,l} R_{m_l}[n-q] + z_t^c[n], n \in [0, T_m - 1]. \tag{44}$$

Note that this approximation comes from the good cross-correlation properties in (40) of the pseudo-random sequence, and the accuracy of the approximation can be affected by the length of the sequences as well as the specific design scheme.

From (39), it is known that when the beam $\mathbf{f}_{\text{RF},t,l}$ aligns with the strong channel tap of $\mathbf{h}_{\text{DL}}^H[q]$ and satisfies $q = n + bT_m, \forall b \in \mathbb{Z}$, $y_{t,l}[n]$ in (44) can achieve a large value relatively. To determine which beam can align with the strong channel tap and decrease the impact of noise, calculating the

Algorithm 1: Codebook-based Analog Beamforming Design

Input: Transmit power P , DFT codebook \mathcal{F}_{DFT} , and pilot sequences $\{m_l[n]\}_{l=1}^{M_{\text{RF}}}$.

Output: The optimal analog beamforming matrix $\mathbf{F}_{\text{RF}}^{\text{opt}}$.

```

1 for  $t = 1 : \lceil M_t / M_{\text{RF}} \rceil$  do
2   Use  $\mathbf{f}_{\text{RF},t,l} \in \mathcal{F}_{\text{DFT}}, \forall l \in [1, M_{\text{RF}}]$  as analog
   beamforming vector and transmit the signal
   in (41);
3   Pass the received signal in (42) through a bank of
   matched filters to obtain  $y_{t,l}[n]$  in (43);
4   Calculate the power  $r_{t,l}$  in (45);
5 end
6 Sort  $r_{t,l}, \forall t, l$  in descending order and select  $M_{\text{RF}}$ 
   vectors  $\mathbf{f}_{\text{RF},t,l}$  corresponding to the first  $M_{\text{RF}}$  largest
    $r_{t,l}$  to form the optimal beamforming matrix  $\mathbf{F}_{\text{RF}}^{\text{opt}}$ ;

```

power after summing $y_{t,l}[n]$, we can obtain

$$\begin{aligned}
r_{t,l} &= \left| \sum_{n=0}^{T_m-1} y_{t,l}[n] \right|^2 \\
&= \bar{p} \left| \sum_{n=0}^{T_m-1} \left(\sum_{q=0}^Q \mathbf{h}_{\text{DL}}^H[q] \mathbf{f}_{\text{RF},t,l} R_{m_l}[n-q] + z_t^c[n] \right) \right|^2.
\end{aligned} \tag{45}$$

As a result, by searching all M_t beams in the codebook and sorting $r_{t,l}, \forall t, l$ in descending order, M_{RF} vectors $\mathbf{f}_{\text{RF},t,l}$ corresponding to the first M_{RF} largest $r_{t,l}$ will be selected, denoted as $\{\mathbf{f}_{\text{RF},l}^{\text{opt}}\}_{l=1}^{M_{\text{RF}}}$, which are used to form the analog beamforming matrix $\mathbf{F}_{\text{RF}}^{\text{opt}} = [\mathbf{f}_{\text{RF},1}^{\text{opt}}, \dots, \mathbf{f}_{\text{RF},M_{\text{RF}}}^{\text{opt}}] \in \mathbb{C}^{M_t \times M_{\text{RF}}}$.

The above codebook-based analog beamforming design for DAM with hybrid beamforming is summarized in Algorithm 1.

B. Digital Beamforming Design

After determining the analog beamforming matrix, the digital beamforming matrix needs to be further determined, which can be based on the tap-based DAM method introduced earlier. Note that the analog beamforming matrix is already determined here, so this stage is equivalent to the fully digital beamforming design, and the transmitted signal is given by

$$\mathbf{x}[n] = \mathbf{F}_{\text{RF}}^{\text{opt}} \sum_{l=1}^{L'} \mathbf{f}_{\text{BB},l} s[n - \kappa_l]. \tag{46}$$

By substituting (46) to (6), the received signal is given by

$$\begin{aligned}
y[n] &= \sum_{q=0}^Q \mathbf{h}_{\text{DL}}^H[q] \mathbf{x}[n-q] + z[n] \\
&= \sum_{q=0}^Q \mathbf{h}_{\text{DL}}^H[q] \mathbf{F}_{\text{RF}}^{\text{opt}} \sum_{l=1}^{L'} \mathbf{f}_{\text{BB},l} s[n - \kappa_l - q] + z[n].
\end{aligned} \tag{47}$$

By letting the downlink equivalent channel tap $\tilde{\mathbf{h}}_{\text{DL}}^H[q] = \mathbf{h}_{\text{DL}}^H[q] \mathbf{F}_{\text{RF}}^{\text{opt}} \in \mathbb{C}^{1 \times M_{\text{RF}}}$, $y[n]$ can be further expressed as

$$y[n] = \sum_{q=0}^Q \sum_{l=1}^{L'} \tilde{\mathbf{h}}_{\text{DL}}^H[q] \mathbf{f}_{\text{BB},l} s[n - \kappa_l - q] + z[n]. \tag{48}$$

Obviously, it is of the same form as (28), the only difference is that the equivalent channel by considering the effect of analog beamforming is used here, which has a much smaller dimension $M_{\text{RF}} \ll M_t$. Therefore, the complexity of channel estimation can be effectively reduced. Assume that the equivalent channel is estimated, with $\mathbf{g}_l^H[i]$ defined in (30), the resulting SINR is given by

$$\gamma = \frac{\left| \sum_{l=1}^{L'} \tilde{\mathbf{h}}_{\text{DL}}^H[q_l] \mathbf{f}_{\text{BB},l} \right|^2}{\sum_{i=-Q, i \neq 0}^Q \left| \sum_{l=1}^{L'} \mathbf{g}_l^H[i] \mathbf{f}_{\text{BB},l} \right|^2 + \sigma^2}. \quad (49)$$

To maximize the spectral efficiency, it is equivalent to maximizing the SINR in (49), which can be written as

$$\begin{aligned} \max_{\{\mathbf{f}_{\text{BB},l}\}_{l=1}^{L'}} & \frac{\left| \sum_{l=1}^{L'} \tilde{\mathbf{h}}_{\text{DL}}^H[q_l] \mathbf{f}_{\text{BB},l} \right|^2}{\sum_{i=-Q, i \neq 0}^Q \left| \sum_{l=1}^{L'} \mathbf{g}_l^H[i] \mathbf{f}_{\text{BB},l} \right|^2 + \sigma^2} \\ \text{s.t.} & \quad \|\mathbf{F}_{\text{RF}}^{\text{opt}} \mathbf{F}_{\text{BB}}\|_F^2 = \sum_{l=1}^L \|\mathbf{F}_{\text{RF}}^{\text{opt}} \mathbf{f}_{\text{BB},l}\|_F^2 \leq P. \end{aligned} \quad (50)$$

Note that the power constraints of this optimization problem include $\mathbf{F}_{\text{RF}}^{\text{opt}}$ which is determined, not just only $\mathbf{f}_{\text{BB},l}$, making the solution in (33) inapplicable here. To this end, let $\mathbf{F}_{\text{RF}}^{\text{opt}} \mathbf{f}_{\text{BB},l} = \mathbf{v}_l$. From the previous section, it can be seen that the columns $\{\mathbf{f}_{\text{RF},l}^{\text{opt}}\}_{l=1}^{M_{\text{RF}}}$ that make up $\mathbf{F}_{\text{RF}}^{\text{opt}}$ are different, each corresponding to a different AoD. Therefore, they are linearly independent, meaning $\mathbf{F}_{\text{RF}}^{\text{opt}}$ is of full column rank. Thus, the digital beamforming vector can be expressed as $\mathbf{f}_{\text{BB},l} = (\mathbf{F}_{\text{RF}}^{\text{opt}})^\dagger \mathbf{v}_l, \forall l$, where $(\mathbf{F}_{\text{RF}}^{\text{opt}})^\dagger$ is the pseudo-inverse of $\mathbf{F}_{\text{RF}}^{\text{opt}}$. Then, the SINR in (49) can be further expressed as

$$\begin{aligned} \gamma &= \frac{\left| \sum_{l=1}^{L'} \tilde{\mathbf{h}}_{\text{DL}}^H[q_l] (\mathbf{F}_{\text{RF}}^{\text{opt}})^\dagger \mathbf{v}_l \right|^2}{\sum_{i=-Q, i \neq 0}^Q \left| \sum_{l=1}^{L'} \mathbf{g}_l^H[i] (\mathbf{F}_{\text{RF}}^{\text{opt}})^\dagger \mathbf{v}_l \right|^2 + \sigma^2} \\ &= \frac{\bar{\mathbf{v}}^H \bar{\mathbf{h}}_{\text{DL}} \bar{\mathbf{h}}_{\text{DL}}^H \bar{\mathbf{v}}}{\bar{\mathbf{v}}^H \left(\sum_{i=-Q, i \neq 0}^Q \bar{\mathbf{g}}[i] \bar{\mathbf{g}}^H[i] + \sigma^2 \mathbf{I} / \|\bar{\mathbf{v}}\|^2 \right) \bar{\mathbf{v}}}, \end{aligned} \quad (51)$$

where $\bar{\mathbf{h}}_{\text{DL}} = [\tilde{\mathbf{h}}_{\text{DL}}^T[q_1]((\mathbf{F}_{\text{RF}}^{\text{opt}})^\dagger)^*, \dots, \tilde{\mathbf{h}}_{\text{DL}}^T[q_{L'}]((\mathbf{F}_{\text{RF}}^{\text{opt}})^\dagger)^*]^T \in \mathbb{C}^{M_t L' \times 1}$, $\bar{\mathbf{v}} = [\mathbf{v}_1^T, \dots, \mathbf{v}_{L'}^T]^T \in \mathbb{C}^{M_t L' \times 1}$, and $\bar{\mathbf{g}}[i] = [\mathbf{g}_1^T[i]((\mathbf{F}_{\text{RF}}^{\text{opt}})^\dagger)^*, \dots, \mathbf{g}_{L'}^T[i]((\mathbf{F}_{\text{RF}}^{\text{opt}})^\dagger)^*]^T \in \mathbb{C}^{M_t L' \times 1}$. Thus, the problem in (50) is equivalent to

$$\begin{aligned} \max_{\bar{\mathbf{v}}} & \frac{\bar{\mathbf{v}}^H \bar{\mathbf{h}}_{\text{DL}} \bar{\mathbf{h}}_{\text{DL}}^H \bar{\mathbf{v}}}{\bar{\mathbf{v}}^H \left(\sum_{i=-Q, i \neq 0}^Q \bar{\mathbf{g}}[i] \bar{\mathbf{g}}^H[i] + \sigma^2 \mathbf{I} / \|\bar{\mathbf{v}}\|^2 \right) \bar{\mathbf{v}}} \\ \text{s.t.} & \quad \|\bar{\mathbf{v}}\|^2 = P. \end{aligned} \quad (52)$$

It is noted that the objective function is a generalized Rayleigh quotient with respect to $\bar{\mathbf{v}}$, which is maximized by the MMSE beamforming $\bar{\mathbf{v}}^{\text{MMSE}} = \sqrt{P} \mathbf{C}^{-1} \bar{\mathbf{h}}_{\text{DL}} / \|\mathbf{C}^{-1} \bar{\mathbf{h}}_{\text{DL}}\|$, where $\mathbf{C} \triangleq \sum_{i=-Q, i \neq 0}^Q \bar{\mathbf{g}}[i] \bar{\mathbf{g}}^H[i] + \sigma^2 \mathbf{I} / P$. Therefore, the optimal digital beamforming vector can be obtained as $\mathbf{f}_{\text{BB},l}^{\text{MMSE}} = (\mathbf{F}_{\text{RF}}^{\text{opt}})^\dagger \mathbf{v}_l^{\text{MMSE}}$.

V. DAM-OFDM WITH HYBRID BEAMFORMING

As discussed in previous sections, for channels with fractional delays, since adjacent channel taps in one cluster have strong correlations, DAM may not completely eliminate ISI. The work in [36] proposed DAM-OFDM, which integrates DAM to flexibly manipulate the channel delay spread for more

efficient OFDM transmission. Inspired by this, it is possible to align each cluster into one cluster using DAM, thereby reducing channel delay spread, and further overcoming the residual ISI with OFDM. To reduce hardware cost and power consumption, hybrid analog/digital beamforming will also be used for DAM-OFDM in the following.

Based on the transmitter architecture of DAM-OFDM with hybrid beamforming in Fig. 3, after OFDM processing, the n th sample of the m th OFDM symbol in the time-domain is given by [36]

$$\bar{\mathbf{x}}_t[m, n] = \frac{1}{\sqrt{K}} \sum_{k=0}^{K-1} \mathbf{u}_k s[m, k] e^{j \frac{2\pi}{K} kn}, \quad n = -N_{\text{CP}}, \dots, K-1, \quad (53)$$

where K is the number of sub-carriers used in OFDM, $\mathbf{u}_k \in \mathbb{C}^{M_u \times 1}$ denotes the digital baseband beamforming vector for sub-carrier k , $s[m, k]$ denotes the information symbol carried by the k th sub-carrier in the m th OFDM symbol, and N_{CP} denotes the length of CP. With parallel to serial conversion, the samples of all OFDM symbols $\bar{\mathbf{x}}_t[m, n]$ are concatenated as a time-domain sequence, which is given by

$$\bar{\mathbf{d}}[i] \triangleq \bar{\mathbf{x}}_t[m, n], \quad \forall n \in [-N_{\text{CP}}, K-1], \quad (54)$$

where $i = m(K + N_{\text{CP}}) + n$. After DAM processing with hybrid beamforming, the transmitted signal is given by

$$\bar{\mathbf{d}}[i] = \mathbf{F}_{\text{RF}} \sum_{l=1}^{L'} \mathbf{F}_{\text{BB},l} \mathbf{d}[i - \kappa_l]. \quad (55)$$

Based on the idea of hybrid beamforming in the previous sections, it is required to design the fully digital beamforming matrix first. Hence we let $\mathbf{F}_l = \mathbf{F}_{\text{RF}} \mathbf{F}_{\text{BB},l} \in \mathbb{C}^{M_t \times M_u}$. Thus, the transmitted signal can be further given by

$$\bar{\mathbf{d}}[i] = \sum_{l=1}^{L'} \mathbf{F}_l \mathbf{d}[i - \kappa_l]. \quad (56)$$

It follows from [36] that the transmit power of $\bar{\mathbf{d}}[i]$ in (56) is

$$\mathbb{E} \left[\|\bar{\mathbf{d}}[i]\|^2 \right] = \frac{1}{K} \sum_{k=0}^{K-1} \left\| \sum_{l=1}^{L'} \mathbf{F}_l \mathbf{u}_k e^{-j \frac{2\pi}{K} k \kappa_l} \right\|^2. \quad (57)$$

Because adjacent taps may exhibit strong correlations under fractional delay conditions, according to subsection III-B, channel taps are grouped into L' clusters. The taps in each cluster are considered to have strong channel correlation. Let $q_l, l = 1, \dots, L'$ be the strongest tap within the l th cluster and align them to the tap $q_{\text{max}} = \max_{1 \leq l \leq L'} q_l$, i.e., let $\kappa_l = q_{\text{max}} - q_l$. Note that the MMSE beamforming will not be used here, as we aim to align all clusters to the cluster with the maximum delay q_{max} with the cluster-based ZF beamforming. Let $\bar{\mathcal{Q}}_l$ denotes the set of taps contained in the l th cluster, where $l \in [1, L']$. Then, for the l th cluster, the set of taps contained in other clusters is denoted by \mathcal{Q}_l . If the absolute value of the maximum difference between the taps and q_l in the l th cluster is $\bar{n}_{l, \text{span}} \triangleq \max_{q \in \bar{\mathcal{Q}}_l} |q - q_l|$, let $\bar{n}_{\text{span}} \triangleq \max_{1 \leq l \leq L'} \bar{n}_{l, \text{span}}$. Thus, the channel delay spread after the alignment of the clusters is around but not larger than $n'_{\text{span}} = 2\bar{n}_{\text{span}}$, which is generally no larger than the original channel delay spread n_{span} , i.e., $n'_{\text{span}} \leq n_{\text{span}}$.

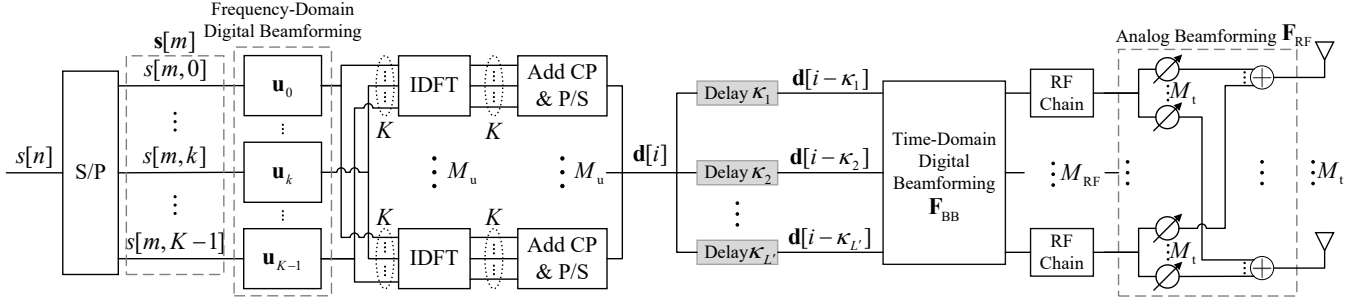


Fig. 3: Transmitter architecture of the DAM-OFDM communication system with hybrid beamforming.

Through the tap-based channel in (6), the received signal is

$$\begin{aligned} y[i] &= \sum_{q=0}^Q \mathbf{h}_{\text{DL}}^H[q] \bar{\mathbf{d}}[i-q] + z[i] \\ &= \sum_{q=0}^Q \sum_{l=1}^{L'} \mathbf{h}_{\text{DL}}^H[q] \mathbf{F}_l \mathbf{d}[i-q-\kappa_l] + z[i]. \end{aligned} \quad (58)$$

Suppose that the strength of the channel taps that are not categorized as clusters are approximated as zero, and let $\kappa_l = q_{\text{max}} - q_l$, $y[i]$ can be further expressed as

$$\begin{aligned} y[i] &= \sum_{l=1}^{L'} \sum_{q \in \bar{Q}_l} \mathbf{h}_{\text{DL}}^H[q] \mathbf{F}_l \mathbf{d}[i - q_{\text{max}} + (q_l - q)] \\ &\quad + \sum_{l=1}^{L'} \sum_{q \in \bar{Q}_l} \mathbf{h}_{\text{DL}}^H[q] \mathbf{F}_l \mathbf{d}[i - q_{\text{max}} + (q_l - q)] + z[i]. \end{aligned} \quad (59)$$

Since in the first term of (59), $q \in \bar{Q}_l$, and thus $(q_l - q) \in [-n'_{\text{span}}/2, n'_{\text{span}}/2]$, the first term represents the taps that is aligned to the cluster containing q_{max} , and the second term represents the term that needs to be forced to zero. Define $\bar{\mathbf{H}}_l \in \mathbb{C}^{M_t \times |\bar{Q}_l|} \triangleq [\mathbf{h}_{\text{DL}}^H[q]]_{q \in \bar{Q}_l}$. To design \mathbf{F}_l so that the second term in (59) can be eliminated, we should have

$$\bar{\mathbf{H}}_l^H \mathbf{F}_l = \mathbf{0}_{|\bar{Q}_l| \times M_u}. \quad (60)$$

This ZF conditions are feasible as long as $\bar{\mathbf{H}}_l^H$ has a non-empty null-space [36]. In this case, the beamforming matrix can be expressed as $\mathbf{F}_l = \bar{\mathbf{H}}_l^\perp \bar{\mathbf{X}}_l$, where $\bar{\mathbf{H}}_l^\perp \in \mathbb{C}^{M_t \times \bar{r}_l}$ denotes an orthonormal basis for the orthogonal complement of $\bar{\mathbf{H}}_l$, and $\bar{\mathbf{X}}_l \in \mathbb{C}^{\bar{r}_l \times M_u}$ is the new beamforming matrix to be designed, with $\bar{r}_l = \text{rank}(\bar{\mathbf{H}}_l^\perp)$. Thus, the received signal in (59) is

$$y[i] = \sum_{l=1}^{L'} \sum_{q \in \bar{Q}_l} \mathbf{h}_{\text{DL}}^H[q] \bar{\mathbf{H}}_l^\perp \bar{\mathbf{X}}_l \mathbf{d}[i - q_{\text{max}} + (q_l - q)] + z[i]. \quad (61)$$

To show the impact of the resulting delay spread more clearly, those components with common delays should be grouped. To this end, for any $t \in [-n'_{\text{span}}/2, n'_{\text{span}}/2]$, define the following effective channel vector

$$\mathbf{g}_l^H[t] = \begin{cases} \mathbf{h}_{\text{DL}}^H[q], & \text{if } \exists q \in \bar{Q}_l, \text{ s.t. } q + \kappa_l = t + q_{\text{max}}, \\ 0, & \text{otherwise.} \end{cases} \quad (62)$$

Thus, (61) can be equivalently written as [36]

$$y[i] = \sum_{t=-n'_{\text{span}}/2}^{n'_{\text{span}}/2} \left(\sum_{l=1}^{L'} \mathbf{g}_l^H[t] \bar{\mathbf{H}}_l^\perp \bar{\mathbf{X}}_l \right) \mathbf{d}[i-t] + z[i]. \quad (63)$$

It is observed from (63) the signal $\mathbf{d}[i]$ would see an effective channel with channel delay spread $n'_{\text{span}} \leq n_{\text{span}}$, after the DAM processing. It is known from [36] that, for DAM-OFDM with $N_{\text{CP}} \geq n'_{\text{span}}$, after removing the CP from the received signal in (61) and performing serial to parallel conversion, it can be further obtained

$$\begin{aligned} y[m, n] &= \frac{1}{\sqrt{K}} \sum_{k=0}^{K-1} \left(\sum_{t=-n'_{\text{span}}/2}^{n'_{\text{span}}/2} \left(\sum_{l=1}^{L'} \mathbf{g}_l^H[t] \bar{\mathbf{H}}_l^\perp \bar{\mathbf{X}}_l \right) e^{-j \frac{2\pi}{K} kt} \right) \\ &\quad \times \mathbf{u}_k s[m, k] e^{j \frac{2\pi}{K} kn} + z[m, n], \forall n \in [0, K-1]. \end{aligned} \quad (64)$$

Let $\tilde{\mathbf{h}}^H[k]$ denotes the equivalent frequency-domain channel of the k th sub-carrier for DAM-OFDM, which is given by

$$\tilde{\mathbf{h}}^H[k] = \frac{1}{\sqrt{K}} \sum_{t=-n'_{\text{span}}/2}^{n'_{\text{span}}/2} \left(\sum_{l=1}^{L'} \mathbf{g}_l^H[t] \bar{\mathbf{H}}_l^\perp \bar{\mathbf{X}}_l \right) e^{-j \frac{2\pi}{K} kt}, \forall k, \quad (65)$$

where the coefficient $1/\sqrt{K}$ is introduced to ensure the conservation of energy between DFT and IDFT. Thus, the received signal in the frequency-domain can be obtained by taking the DFT to (64), which is given by

$$y_t[m, k] = \sqrt{K} \tilde{\mathbf{h}}^H[k] \mathbf{u}_k s[m, k] + z[m, k], \forall k \in [0, K-1]. \quad (66)$$

Therefore, the received SNR for sub-carrier k is

$$\begin{aligned} \gamma_k &= K \left| \tilde{\mathbf{h}}^H[k] \mathbf{u}_k \right|^2 / \sigma^2 \\ &= \frac{\left| \sum_{t=-n'_{\text{span}}/2}^{n'_{\text{span}}/2} \left(\sum_{l=1}^{L'} \mathbf{g}_l^H[t] \bar{\mathbf{H}}_l^\perp \bar{\mathbf{X}}_l \right) e^{-j \frac{2\pi}{K} kt} \mathbf{u}_k \right|^2}{\sigma^2}. \end{aligned} \quad (67)$$

As a result, the spectral efficiency of DAM-OFDM can be maximized by jointly optimizing the time-domain beamforming matrices $\{\bar{\mathbf{X}}_l\}_{l=1}^{L'}$ and the frequency-domain beamforming vectors $\{\mathbf{u}_k\}_{k=0}^{K-1}$ with the dimension M_u . The optimization problem can be formulated as

$$\begin{aligned} \max_{\{\bar{\mathbf{X}}_l\}_{l=1}^{L'}, \{\mathbf{u}_k\}_{k=0}^{K-1}, M_u} & \frac{1}{K} \sum_{k=0}^{K-1} \log_2(1 + \gamma_k) \\ \text{s.t.} & \sum_{k=0}^{K-1} \left\| \sum_{l=1}^{L'} \bar{\mathbf{H}}_l^\perp \bar{\mathbf{X}}_l \mathbf{u}_k e^{-j \frac{2\pi}{K} k \kappa_l} \right\|^2 \leq KP. \end{aligned} \quad (68)$$

This problem can be solved using the methods outlined in steps 3 to 5 of Algorithm 1 in [36]. Note that M_u can be chosen flexibly to obtain the optimal solution, which is denoted by $\{\bar{\mathbf{X}}_l^{\text{opt}}\}_{l=1}^{L'}$ and $\{\mathbf{u}_k^{\text{opt}}\}_{k=0}^{K-1}$. Finally, to implement

TABLE I: Parameter settings

Parameter	value
Number of RF chains	$M_{\text{RF}} = 4$
Carrier frequency	$f = 28\text{GHz}$
Total bandwidth	$B = 128\text{MHz}$
Noise power spectral density	$N_0 = -174\text{dBm/Hz}$
Inter-element spacing of the ULA	$d = \lambda/2$
Channel coherence time	$T_c = 1\text{ms}$
Number of temporal-resolvable multi-paths	$L = 4$
Delay	$\tau_l \sim U[0, \tau_{\text{max}}], \tau_{\text{max}} = 312.5\text{ns}$
Number of sub-paths	$\mu_l \sim U[0, \mu_{\text{max}}], \mu_{\text{max}} = 3$
AoDs	$\theta_{li} \sim U[-60^\circ, 60^\circ], \forall l, i$
Number of sub-carriers used in OFDM	$K = 256$
Threshold for selecting significant taps	$C = 0.01$

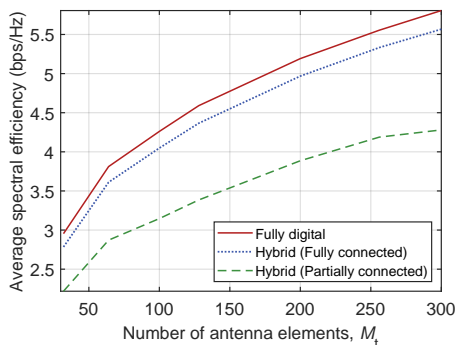


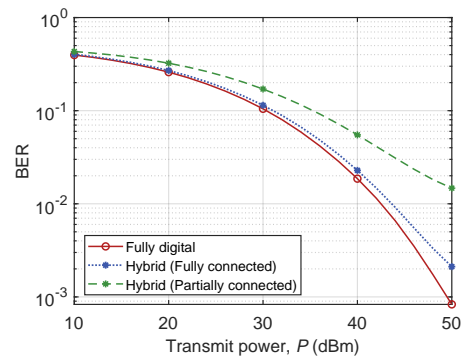
Fig. 4: Spectral efficiency of DAM for channels with integer delays.

DAM-OFDM based on hybrid analog/digital beamforming, according to the method in Section III, analog beamforming matrix \mathbf{F}_{RF} and digital beamforming matrix $\mathbf{F}_{\text{BB},l}$ need to be designed so that $\mathbf{F}_{\text{RF}}\mathbf{F}_{\text{BB},l}$ is as close to $\mathbf{F}_l = \mathbf{H}_l^\perp \bar{\mathbf{X}}_l^{\text{opt}}$ as possible, which can be achieved using the OMP algorithm.

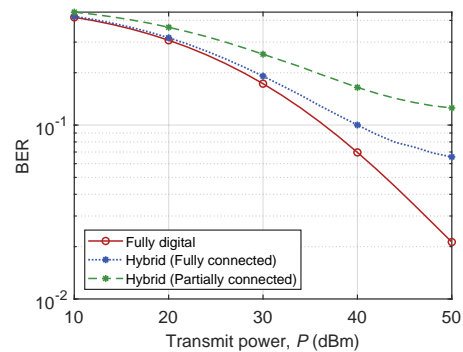
VI. SIMULATION RESULTS

In this section, simulation results are provided to verify the effectiveness of the proposed hybrid beamforming designs for DAM. Unless otherwise stated, the parameter settings of the simulation results are summarized in Table I. Furthermore, the coefficient $\alpha_l, \forall l$ in (3) are generated using the model developed in [34].

For transmit power of $P = 30$ dBm, Fig. 4 illustrates the average spectral efficiency versus the number of antenna elements M_t for DAM based on fully digital and hybrid beamforming. It can be observed that when the number of RF chains is 4, which is equal to that of multi-paths, the average spectral efficiency of DAM based on fully digital beamforming and that of DAM based on hybrid beamforming with fully connected structure exhibit an increasing trend with similar rates of growth as the number of transmit antennas increases. This is because the ability of hybrid beamforming to approach the performance of fully digital beamforming depends mainly on the number of RF chains, rather than the number of transmit antennas. However, the average spectral efficiency of DAM based on hybrid beamforming with the fully connected



(a) Integer delays



(b) Fractional delays

Fig. 5: BER performance of DAM for channels with integer delays and fractional delays.

structure is slightly lower than that based on fully digital beamforming. This is attributed to the unit modulus constraint imposed on the analog beamforming matrix in the hybrid scheme. Furthermore, the average spectral efficiency of hybrid beamforming with the partially connected structure is clearly inferior to that with the fully connected structure, which is due to the fact that the partially connected structure restricts each RF chain to be connected to a subset of antennas, reducing the degrees of freedom in beamforming. However, while hybrid beamforming suffers from some performance losses compared to fully digital beamforming, it offers a trade-off by reducing cost and hardware complexity.

Fig. 5 shows the bit error rate (BER) performance comparison of DAM based on fully digital beamforming versus hybrid beamforming for channels with integer delays as well as fractional delays, respectively. The simulation results are obtained based on Monte Carlo simulations. Specifically, we simulate the transmission process of random bit sequences of length 10^5 using 128-QAM over the randomly generated channels 10^3 times, and the BER is obtained by taking the average over all transmissions. The number of antennas is $M_t = 256$. Fig. 5 reveals that, when the number of RF chains is $N_{\text{RF}} = 4$, which is equal to that of multi-paths, the BER performance of DAM based on hybrid beamforming with fully connected structure is quite close to that based on fully digital beamforming, while the BER performance of that based on hybrid beamforming with partially-connected structure is

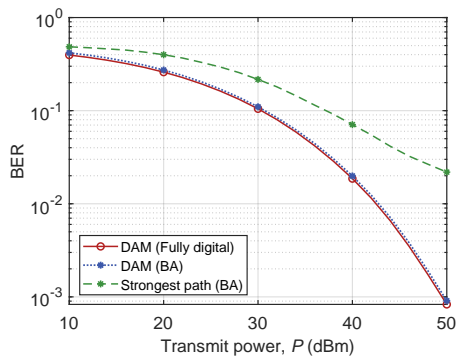


Fig. 6: BER comparison for DAM with beam alignment and fully digital beamforming, as well as the benchmarking strongest path scheme.

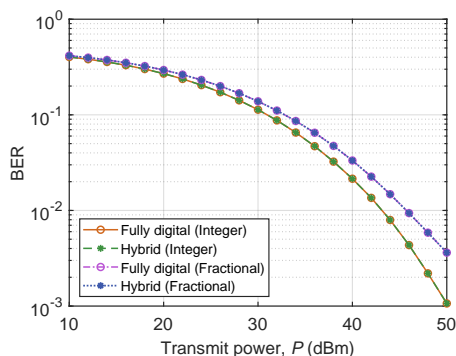


Fig. 7: BER comparison of DAM-OFDM based on fully digital beamforming versus hybrid beamforming for channels with integer delays as well as fractional delays.

clearly worse. Furthermore, comparing Fig. 5a and Fig. 5b, it is apparent that DAM performs worse in channels with fractional delays than in channels with integer delays. This is due to the strong correlation between adjacent taps, which leads to ISI that cannot be completely eliminated, resulting in the occurrence of a BER floor as the transmit power increases.

Fig. 6 compares the BER performance of DAM with beam alignment (BA) and fully digital beamforming, as well as the benchmarking strongest path scheme. The number of RF chains used here is 16, and the fully connected structure is considered. It can be seen that the performance of DAM with beam alignment is identical to that of DAM with fully digital beamforming. This validates the efficacy of beam alignment design for DAM, indicating its practical application in mmWave/THz massive MIMO communication scenarios. It can also be clearly seen from Fig. 6 that the performance of benchmarking strongest path is worse than DAM, which is due to the fact that it only utilizes one channel tap, failing to fully utilize the channel or losing diversity, verifying that the DAM brings performance advantages due to its ability to fully utilize the channel power contributed by all multi-path components.

Fig. 7 presents the BER performance comparison of DAM-OFDM based on fully digital beamforming versus hybrid

beamforming for channels with integer delays as well as fractional delays. The number of RF chains used here is 16, and it can be seen that when the number of RF chains is large enough, the performance of DAM-OFDM based on hybrid beamforming is almost equal to that based on fully digital beamforming. It can also be seen from Fig. 7 that, unlike what is presented in Fig. 5, there is only a small degradation in the performance of DAM-OFDM over the channel with fractional delays as compared to that with integer delays. This is due to the fact that OFDM is able to further overcome ISI after DAM reduces the delay spread. The slight degradation is due to the correlation between different taps of the channel with fractional delays, which causes some performance loss in DAM with ZF beamforming. Nevertheless, the reduced delay spread due to DAM allows for a reduction in the use of OFDM sub-carriers or CP [36].

VII. CONCLUSION

This paper proposed the hybrid analog/digital beamforming-based DAM for mmWave/THz communications, including fully connected and partially connected structures. It leverages the high spatial resolution of large antenna arrays and the sparsity of multi-paths in mmWave/THz channels to mitigate ISI, with much fewer RF chains than the number of antennas. The beam codebook based beam alignment DAM was further proposed, which can reduce the overhead and complexity of channel estimation. Furthermore, for channels with fractional delays, the proposed DAM-OFDM with hybrid beamforming method leverages first DAM to reduce delay spread and then OFDM to cope with the residual ISI, thus significantly reducing the number of OFDM sub-carriers and CP length. Simulation results verified the effectiveness of the proposed methods.

REFERENCES

- [1] H. Lu, Y. Zeng, C. You, Y. Han, J. Zhang, Z. Wang, Z. Dong, S. Jin, C. Wang, T. Jiang, X. You and R. Zhang, "A tutorial on near-field XL-MIMO communications towards 6G," *IEEE Commun. Surv. Tutorials*, 2024.
- [2] D. Moltchanov, E. Sopin, V. Begishev, A. Samuylov, Y. Koucheryavy and K. Samouylov, "A tutorial on mathematical modeling of 5G/6G millimeter wave and terahertz cellular systems," *IEEE Commun. Surv. Tutorials*, vol. 24, no. 2, pp. 1072-1116, 2nd Quart. 2022.
- [3] P. Jain, A. Gupta, N. Kumar and M. Guizani, "Dynamic and efficient spectrum utilization for 6G with THz, mmWave, and RF band," *IEEE Trans. Veh. Technol.*, vol. 72, no. 3, pp. 3264-3273, Mar. 2023.
- [4] R. W. Heath Jr and A. Lozano, *Foundations of MIMO communication*. Cambridge, U.K.: Cambridge Univ. Press, 2018.
- [5] A. Goldsmith, *Wireless communications*. Cambridge, U.K.: Cambridge Univ. Press, 2005.
- [6] M. Tuchler, A. C. Singer and R. Koetter, "Minimum mean squared error equalization using a priori information," *IEEE Trans. Signal Process.*, vol. 50, no. 3, pp. 673-683, Mar. 2002.
- [7] T. M. Hollis, D. J. Comer and D. T. Comer, "Mitigating ISI through self-calibrating continuous-time equalization," *IEEE Trans. Circuits Syst. I Regul. Pap.*, vol. 53, no. 10, pp. 2234-2245, Oct. 2006.
- [8] J. E. Smee and N. C. Beaulieu, "Error-rate evaluation of linear equalization and decision feedback equalization with error propagation," *IEEE Trans. Commun.*, vol. 46, no. 5, pp. 656-665, May 1998.
- [9] X. Xia, "New precoding for intersymbol interference cancellation using nonmaximally decimated multirate filterbanks with ideal FIR equalizers," *IEEE Trans. Signal Process.*, vol. 45, no. 10, pp. 2431-2441, Oct. 1997.

- [10] H. Harashima and H. Miyakawa, "Matched-transmission technique for channels with intersymbol interference," *IEEE Trans. Commun.*, vol. 20, no. 4, pp. 774–780, Aug. 1972.
- [11] M. Fink, "Time reversal of ultrasonic fields. I. Basic principles," *IEEE Trans. Ultrason. Ferroelectr. Freq. Control*, vol. 39, no. 5, pp. 555–566, Sept. 1992.
- [12] R. C. Qiu, C. Zhou, N. Guo and J. Q. Zhang, "Time reversal with MISO for ultrawideband communications: Experimental results," *IEEE Antennas Wirel. Propag. Lett.*, vol. 5, pp. 269–273, 2006.
- [13] M. Emami, M. Vu, J. Hansen, A. J. Paulraj, and G. Papanicolaou, "Matched filtering with rate back-off for low complexity communications in very large delay spread channels," in *Proc. 38th Asilomar Conf. Signals, Syst. Comput.*, vol. 1, 2004, pp. 218–222.
- [14] B. Wang, Y. Wu, F. Han, Y. Yang, and K. R. Liu, "Green wireless communications: A time-reversal paradigm," *IEEE J. Sel. Areas Commun.*, vol. 29, no. 8, pp. 1698–1710, Sep. 2011.
- [15] M. Z. Win and Z. A. Kostic, "Virtual path analysis of selective Rake receiver in dense multipath channels," *IEEE Commun. Lett.*, vol. 3, no. 11, pp. 308–310, Nov. 1999.
- [16] Y. Liang and J. M. Cioffi, "Combining transmit beamforming, space-time block coding and delay spread reduction," in *Proc. 14th IEEE Proc. Pers., Indoor Mobile Radio Commun.*, vol. 1, 2003, pp. 105–109.
- [17] Y. Liang, F. Chin and W. Leon, "Statistical pre-filtering for OFDM systems with multiple transmit antennas," in *Proc. IEEE 60th Veh. Technol. Conf.*, vol. 2, 2004, pp. 1498–1502.
- [18] W. Leon and Y. Liang, "Statistical pre-filtering for MIMO-OFDM systems," in *Proc. IEEE 61st Veh. Technol. Conf.*, vol. 2, 2005, pp. 1012–1016.
- [19] D. Falconer, S. L. Ariyavisitakul, A. Benyamin-Seeyar and B. Eidson, "Frequency domain equalization for single-carrier broadband wireless systems," *IEEE Commun. Mag.*, vol. 40, no. 4, pp. 58–66, Apr. 2002.
- [20] H. Sari, G. Karam and I. Jeanclaude, "Frequency-domain equalization of mobile radio and terrestrial broadcast channels," in *Proc. IEEE GLOBECOM*, 1994, pp. 1–5.
- [21] Y. Zhu and K. Ben Letaief, "Single-carrier frequency-domain equalization with noise prediction for MIMO systems," *IEEE Trans. Commun.*, vol. 55, no. 5, pp. 1063–1076, May 2007.
- [22] L. Cimini, "Analysis and simulation of a digital mobile channel using orthogonal frequency division multiplexing," *IEEE Trans. Commun.*, vol. 33, no. 7, pp. 665–75, Jul. 1985.
- [23] S. H. Han and J. H. Lee, "An overview of peak-to-average power ratio reduction techniques for multicarrier transmission," *IEEE Wireless Commun.*, vol. 12, no. 2, pp. 56–65, Apr. 2005.
- [24] Y. Hung and S. L. Tsai, "PAPR analysis and mitigation algorithms for beamforming MIMO OFDM systems," *IEEE Trans. Wireless Commun.*, vol. 13, no. 5, pp. 2588–2600, May 2014.
- [25] B. Farhang-Boroujeny, "OFDM versus filter bank multicarrier," *IEEE Signal Process. Mag.*, vol. 28, no. 3, pp. 92–112, May 2011.
- [26] Y. Yao and G. B. Giannakis, "Blind carrier frequency offset estimation in SISO, MIMO, and multiuser OFDM systems," *IEEE Trans. Commun.*, vol. 53, no. 1, pp. 173–183, Jan. 2005.
- [27] R. Hadani, S. Rakib, M. Tsatsanis, A. Monk, A. J. Goldsmith, A. F. Molisch and R. Calderbank, "Orthogonal time frequency space modulation," in *Proc. IEEE Wireless Commun. Netw. Conf. (WCNC)*, 2017, pp.1–6.
- [28] Z. Wei, W. Yuan, S. Li, J. Yuan, G. Bharatula, R. Hadani, and L. Hanzo, "Orthogonal time-frequency space modulation: A promising next-generation waveform," *IEEE Wireless Commun.*, vol. 28, no. 4, pp. 136–144, Aug. 2021.
- [29] S. Li, J. Yuan, W. Yuan, Z. Wei, B. Bai and D. W. K. Ng, "Performance analysis of coded OTFS systems over high-mobility channels," *IEEE Trans. on Wireless Commun.*, vol. 20, no. 9, pp. 6033–6048, Sept. 2021.
- [30] H. Lin and J. Yuan, "Orthogonal delay-doppler division multiplexing modulation," *IEEE Trans. Wireless Commun.*, vol. 21, no. 12, pp. 11024–11037, Dec. 2022.
- [31] H. Lu and Y. Zeng, "Delay alignment modulation: Enabling equalization-free single-carrier communication," *IEEE Wireless Commun. Lett.*, vol. 11, no. 9, pp. 1785–1789, Sept. 2022.
- [32] S. Chen, S. Sun, G. Xu, X. Su and Y. Cai, "Beam-space multiplexing: Practice, theory, and trends, from 4G TD-LTE, 5G, to 6G and beyond," *IEEE Wireless Commun.*, vol. 27, no. 2, pp. 162–172, Apr. 2020.
- [33] S. Schwarz and S. Pratschner, "Multiple antenna systems in mobile 6G: Directional channels and robust signal processing," *IEEE Commun. Mag.*, vol. 61, no. 4, pp. 64–70, Apr. 2023.
- [34] M. R. Akdeniz, Y. Liu, M. K. Samimi, S. Sun, S. Rangan, T. S. Rappaport and E. Erkip, "Millimeter wave channel modeling and cellular capacity evaluation," *IEEE J. Sel. Areas Commun.*, vol. 32, no. 6, pp. 1164–1179, Jun. 2014.
- [35] Y. Zeng and R. Zhang, "Millimeter wave MIMO with lens antenna array: A new path division multiplexing paradigm," *IEEE Trans. Commun.*, vol. 64, no. 4, pp. 1557–1571, Apr. 2016.
- [36] H. Lu and Y. Zeng, "Delay alignment modulation: Manipulating channel delay spread for efficient single- and multi-carrier communication," *IEEE Trans. Commun.*, vol. 71, no. 11, pp. 6316–6331, Nov. 2023.
- [37] X. Wang, H. Lu and Y. Zeng, "Multi-user delay alignment modulation for millimeter wave massive MIMO," in *Proc. IEEE GLOBECOM*, 2023, pp. 6970–6975.
- [38] X. Wang, H. Lu, Y. Zeng, X. Xu, J. Xu, "Achievable rate region and path-based beamforming for multi-user single-carrier delay alignment modulation," *arXiv preprint arXiv:2309.00391*, 2023.
- [39] H. Lu, Y. Zeng, S. Jin and R. Zhang, "Single-carrier delay alignment modulation for multi-IRS aided communication," *IEEE Trans. Wireless Commun.*, vol. 23, no. 4, pp. 3267–3282, Apr. 2024.
- [40] D. Ding, Y. Zeng and D. Wang, "Channel estimation for delay alignment modulation," in *Proc. 2024 IEEE Wireless Commun. Netw. Conf. (WCNC)*, 2024, pp. 1–6.
- [41] Z. Zhou, Z. Xiao and Y. Zeng, "Fractional delay alignment modulation for spatially sparse wireless communications," in *Proc 2024 IEEE Wireless Commun. Netw. Conf. (WCNC)*, 2024, pp. 1–6.
- [42] Z. Xiao and Y. Zeng, "Integrated Sensing and Communication with Delay Alignment Modulation," in *Proc. IEEE Int. Conf. Commun. (ICC)*, 2022, pp. 1–6.
- [43] Z. Xiao and Y. Zeng, "Integrated sensing and communication with delay alignment modulation: Performance analysis and beamforming optimization," *IEEE Trans. Wireless Comm.*, vol. 22, no. 12, pp. 8904–8918, Apr. 2023.
- [44] Z. Xiao, Y. Zeng, F. Wen, Z. Zhang and D. W. K. Ng, "Integrated sensing and channel estimation by exploiting dual timescales for delay-Doppler alignment modulation," *arXiv preprint arXiv:2310.11326*, 2023.
- [45] Z. Wang, X. Mu and Y. Liu, "Bidirectional integrated sensing and communication: Full-duplex or half-duplex?," *IEEE Trans. Wireless Commun.*, vol. 23, no. 8, pp. 8184–8199, Aug. 2024.
- [46] W. Hao, H. Shi, G. Sun and C. Huang, "Joint beamforming design for active RIS-aided THz ISAC systems with delay alignment modulation," *IEEE Wireless Commun. Lett.*, vol. 12, no. 10, pp. 1816–1820, Oct. 2023.
- [47] G. Sun, H. Shi, B. Shang and W. Hao, "Secure transmission for active RIS-assisted THz ISAC systems with delay alignment modulation," *IEEE Wireless Commun. Lett.*, vol. 28, no. 5, pp. 1019–1023, May 2024.
- [48] H. Lu and Y. Zeng, "Delay-Doppler alignment modulation for spatially sparse massive MIMO communication," *IEEE Trans. Wireless Commun.*, vol. 23, no. 6, pp. 6000–6014, Jun. 2024.
- [49] Z. Xiao, X. Liu, Y. Zeng, J. A. Zhang, S. Jin and R. Zhang, "Rethinking waveform for 6G: Harnessing delay-Doppler alignment modulation," *arXiv preprint arXiv:2406.09190*, 2024.
- [50] X. Liu, Z. Zhou, Z. Xiao and Y. Zeng, "Orthogonal time frequency space with delay-Doppler alignment modulation," *arXiv preprint arXiv:2407.05641*, 2024.
- [51] X. Yu, J. Shen, J. Zhang and K. B. Letaief, "Alternating minimization algorithms for hybrid precoding in millimeter wave MIMO systems," *IEEE J. Sel. Top. Signal Process.*, vol. 10, no. 3, pp. 485–500, Apr. 2016.
- [52] O. E. Ayach, S. Rajagopal, S. Abu-Surra, Z. Pi and R. W. Heath, "Spatially sparse precoding in millimeter wave MIMO systems," *IEEE Trans. Wireless Commun.*, vol. 13, no. 3, pp. 1499–1513, Mar. 2014.
- [53] L. Yan, C. Han and J. Yuan, "A dynamic array-of-subarrays architecture and hybrid precoding algorithms for Terahertz wireless communications," *IEEE J. Sel. Areas Commun.*, vol. 38, no. 9, pp. 2041–2056, Sept. 2020.
- [54] J. Zhang and Y. Zeng, "Delay alignment modulation with hybrid beamforming for spatially sparse communications," in *Proc 2024 IEEE Wireless Commun. Netw. Conf. (WCNC)*, 2024, pp. 1–6.
- [55] E. Zhang and C. Huang, "On achieving optimal rate of digital precoder by RF-baseband codesign for MIMO systems," in *Proc. 2014 IEEE 80th Veh. Technol. Conf. (VTC2014-Fall)*, 2014, pp. 1–5.
- [56] F. Sahrabi and W. Yu, "Hybrid digital and analog beamforming design for large-scale antenna arrays," *IEEE J. Sel. Top. Signal Process.*, vol. 10, no. 3, pp. 501–513, Apr. 2016.
- [57] X. Song, S. Haghighatshoar and G. Caire, "Efficient beam alignment for millimeter wave single-carrier systems with hybrid MIMO transceivers," *IEEE Trans. Wireless Commun.*, vol. 18, no. 3, pp. 1518–1533, Mar. 2019.